



Endometriosis, a common but enigmatic disease with many faces: current concept of pathophysiology, and diagnostic strategy

Mayumi Takeuchi¹ · Kenji Matsuzaki² · Masafumi Harada¹

Received: 26 January 2024 / Accepted: 6 April 2024
© The Author(s) 2024

Abstract

Endometriosis is a benign, common, but controversial disease due to its enigmatic etiopathogenesis and biological behavior. Recent studies suggest multiple genetic, and environmental factors may affect its onset and development. Genomic analysis revealed the presence of cancer-associated gene mutations, which may reflect the neoplastic aspect of endometriosis. The management has changed dramatically with the development of fertility-preserving, minimally invasive therapies. Diagnostic strategies based on these recent basic and clinical findings are reviewed. With a focus on the presentation of clinical cases, we discuss the imaging manifestations of endometriomas, deep endometriosis, less common site and rare site endometriosis, various complications, endometriosis-associated tumor-like lesions, and malignant transformation, with pathophysiologic conditions.

Keywords Endometriosis · Deep endometriosis · Endometrioma · Malignant transformation · Magnetic resonance imaging (MRI)

Introduction

Endometriosis significantly impairs women's quality of life with chronic pain and reduced fertility and has become an important issue from a public health perspective in light of recent lifestyle changes. Endometriosis is a benign, common, but controversial disease due to its enigmatic etiopathogenesis and biological behavior. Recent studies suggest multiple genetic, and environmental factors such as endocrine, inflammatory, immunological, and angiogenetic may affect its onset and development [1–3]. Genomic analysis revealed the presence of cancer-associated gene mutations, which may reflect the neoplastic aspect of endometriosis [1, 3].

Endometriosis affects approximately 10% of women during their reproductive years, meaning that it affects approximately 190 million women worldwide [1, 2]. Endometriosis is a chronic, inflammatory disease characterized by the presence of endometrial-like tissue outside the uterus, and is associated with debilitating painful symptoms in many patients, also at greater risk of infertility [3–6], emergence of fatigue, multisite pain, and other comorbidities. High risk of subsequent development of autoimmune disease, cancer, and cardiovascular disease is also reported [1, 7].

In this article, we reviewed the imaging features of endometriosis and various related conditions.

Causes of endometriosis

In retrograde menstruation, menstrual blood containing endometrial cells with mutation (*ARID1A/PIK3CA*) flows back through the fallopian tubes and into the pelvic cavity [1, 8–10]. These endometrial cells stick to the pelvic walls and surfaces of the pelvic organs, where they grow and continue to thicken and bleed for each menstrual cycle. Endometrioma (endometriotic cyst) may be formed in the ovaries [4, 8, 9, 11].

✉ Mayumi Takeuchi
mayumi@tokushima-u.ac.jp

Kenji Matsuzaki
kenji@kgw.bunri-u.ac.jp

Masafumi Harada
masafumi@tokushima-u.ac.jp

¹ Department of Radiology, Tokushima University, 3-18-15, Kuramoto-Cho, Tokushima 7708503, Japan

² Department of Radiological Technology, Tokushima Bunri University, Sanuki City, ShidoKagawa 1314-17692193, Japan

Other causes implicated in endometriosis include coelomic metaplasia, in which hormonal or immune factors facilitate the conversion of peritoneal cells into endometrial tissue; embryonic cell transformation, in which estrogen could induce the conversion of embryonic cells into endometrial tissue during puberty; surgical scar implantation, in which endometrial cells may adhere to surgical incisions post-surgery, such as after a cesarean section; endometrial cell transport, in which blood vessels or the lymphatic system might ferry endometrial cells to distant sites; and immune system disorders, which may prevent the body from identifying and eliminating endometrial tissue growing outside the uterus [3, 4, 11].

Classification of endometriosis

The revised American Society for Reproductive Medicine (rASRM) classification based on laparoscopic findings is accepted globally and has been widely used [12]. The rASRM is staged according to a point system based on the presence, size (< 1 cm, 1–3 cm, or > 3 cm), and depth (superficial or deep) of ovarian and peritoneal endometriosis, the presence and extent of ovarian and tubal adhesions (filmy or dense), and the degree of posterior cul-de-sac obliteration (partial or complete). The rASRM is easy to explain the degree of endometriosis in simple terms to patients. Disadvantages of rASRM are (1) Difference between histology and laparoscopic diagnosis, (2) The reproducibility is poor, (3) Infertility and severities of pain are not correlated, and (4) The presence of deep endometriosis is not considered [13, 14].

ENZIAN classification is based on laparoscopic findings but could be determined by imaging modalities (US and MRI) [15]. The advantages of ENZIAN classification are (1) A comprehensive minimally invasive and surgical description system for endometriosis, (2) It provides detailed descriptions of the retroperitoneal structures, (3) It can be determined by imaging modalities such as US and MRI, and (4) Localization and extent of endometriosis are associated and correlated with the presence and severity of different symptoms. MRI–ENZIAN correlation has a high accuracy of 95 to 97% for deep endometriosis. However, it has some disadvantages: (1) International acceptance is poor, (2) Patients may not readily understand, (3) Inaccurate if incomplete surgical dissection of deep endometriosis or image study alone is performed, (4) There are not sufficient studies regarding the feasibility of the classification determined by imaging [14, 16–18].

Endometrioma (endometriotic cyst)

Endometriosis is usually seen in the pelvic cavity, especially in the peritoneum, uterine ligaments (the uterosacral, broad, or round), and ovaries. Less commonly, the bowel, ureter, bladder, lymph nodes, and cesarean section scar may be affected. Ovarian endometriomas (endometriotic cysts) are characterized by altered luminal blood as “chocolate cysts” caused by repeated cyclic hemorrhage [4, 5]. Multiple high signal intensity cysts on T1-weighted images (multiplicity), and the shading sign (T2-shortening in adnexal cyst exhibiting T1-high signal intensity) are suggestive findings of endometrioma (Fig. 1) [19–21]. “Shading” may appear as a complete loss of signal or dependent layering with a low signal intensity fluid level on T2-weighted images. The cause of T2-low signal intensity is complex; hyperviscosity and high concentration of protein and hemosiderin from recurrent cyclical bleeding may contribute to T2-shortening [22]. The overall diagnostic value obtained using shading sign (T1-high: \geq fat) and/or multiplicity is a sensitivity of 90%, specificity of 98%, and accuracy of 96% [20]. A follow-up study reported better sensitivity (93%) but low specificity (45%) [23], however, this discrepancy may be due to differences in signal threshold in T1-weighted image (T1-high: \geq skeletal muscle). Lesions that do not show as strong a signal as fat on T1-weighted images may include non-endometrial hemorrhagic cysts, suggesting that specificity may have decreased. Doubling of magnetic susceptibility at 3 T may influence the diagnostic ability. Because susceptibility-induced signal intensity loss may increase from 1.5 T to 3 T, the shading sign is well visualized at 3 T [24]. T2 dark spot sign (T2-low signal intensity clots within the cyst which are often linear, punctate, or oval in shape) is specific for endometrioma with a sensitivity of 36% and specificity of 93% [23].

Deposition of hemosiderin-laden macrophages within the cyst wall due to repeated cyclic hemorrhage is a pathologic feature of endometrioma, and dotted or curved linear signal voids due to hemosiderin deposition along the cyst wall on susceptibility-weighted images (SWI) are suggestive of endometrioma (Figs. 1, 2) [25, 26]. One study reported an overall diagnostic value of accuracy of 97.6% with the combination of the shading sign and SWI [25]. Because signal voids within the cyst may be seen also in non-endometriotic lesions such as hemorrhagic corpus luteum cysts, the presence of signal voids in the cyst wall should be carefully interpreted [26]. Signal voids due to hemosiderin-deposition along the walls of endometriomas on SWI are more prominent at 3 T than at 1.5 T, however, susceptibility artifacts caused by intestinal gas, metallic, or other materials also are more prominent at 3 T [25].

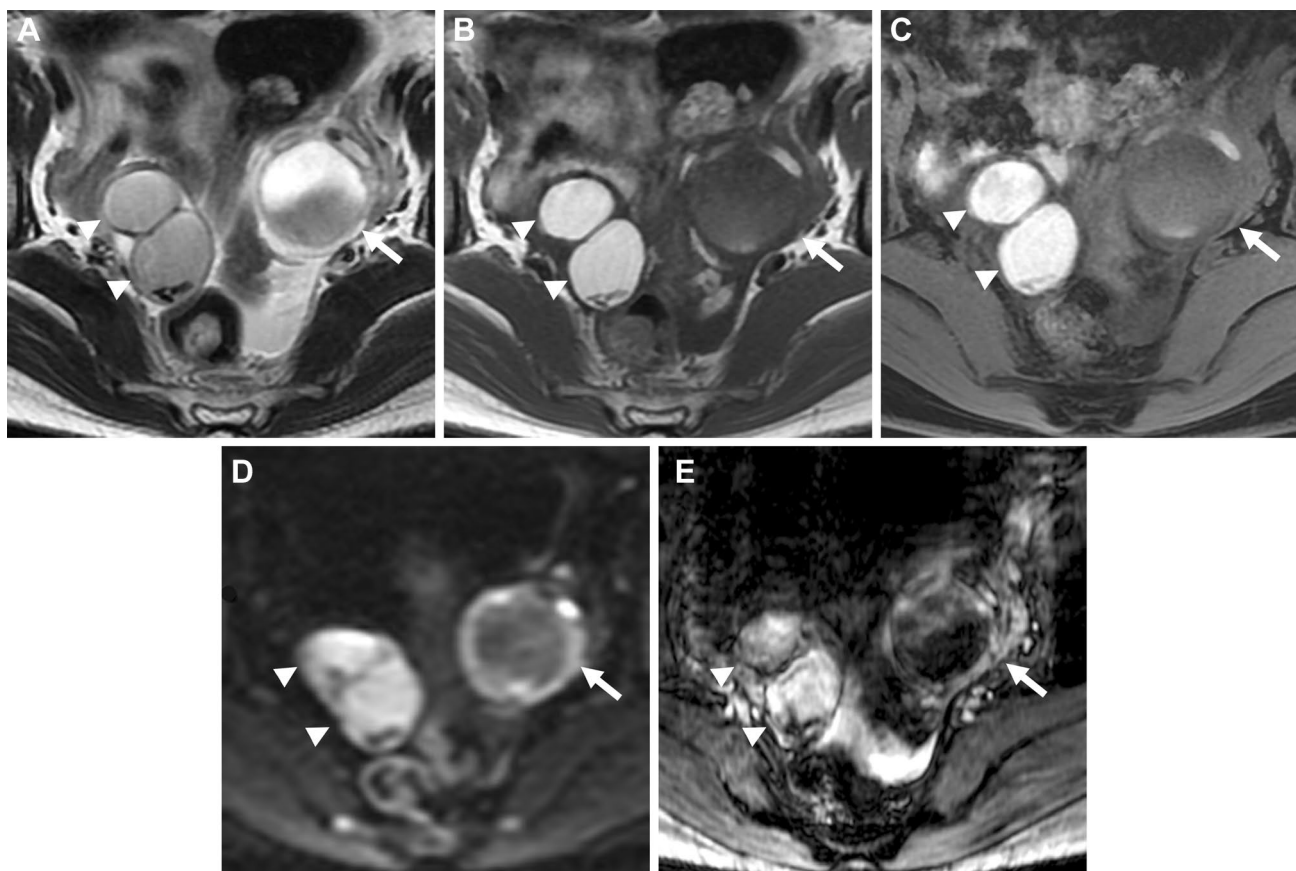


Fig. 1 Endometrioma (typical) and hemorrhagic corpus luteum cyst. A 40-year-old with a history of pelvic pain and suspicion of bilateral ovarian cysts on ultrasonography examination. **A** T2-weighted image reveals bilateral ovarian cysts. The right cysts (arrowheads) show a faint, layered signal loss, whereas the left cyst (arrow) shows a partial signal loss. T2 dark spots are demonstrated in the right posterior cyst. **B** On T1-weighted image, the right cysts show high signal intensity (\geq fat) and the left cyst exhibits low signal intensity. No signal decrease is observed in the right ovarian cysts on **C** fat-saturated T1-weighted image. Multiple T1-high signal intensity cysts (multi-

plicity), the shading sign (T2-shortening in adnexal cyst exhibiting T1-high signal intensity), and the presence of T2 dark spot suggest right ovarian endometriomas. The left cyst is suggestive of the non-endometriotic hemorrhagic cyst (corpus luteum cyst). **D** Diffusion-weighted image (DWI) ($b=800$ s/mm²) shows totally high signal intensity in the right cysts, and ring-like high signal intensity in the left cyst. **E** Susceptibility-weighted image (SWI: susceptibility-weighted angiography) reveals dotty to curved linear signal voids in the walls of the right cysts. Signal voids are prominent within the left cysts but not in the cyst wall

Deep endometriosis/extragenital endometriosis

Deep endometriosis

Deep (infiltrating) endometriosis may cause severe pelvic pain and infertility and is classically defined by the invasion of endometrial tissue at least 5 mm beneath the peritoneal surface [27]. Clinically, “adenomyosis externa” at the rectosigmoid, Douglas' pouch, uterosacral ligament, rectovaginal septum, vesico-uterine pouch, etc. is considered deep endometriosis [28]. Deep endometriosis of the peritoneum, ligaments, or organs may cause solid masses exhibiting T2-low signal intensity and intense contrast enhancement reflecting fibromuscular hyperplasia around sparse ectopic endometrial glands (Fig. 3) [29–35]. The cyclic hemorrhage

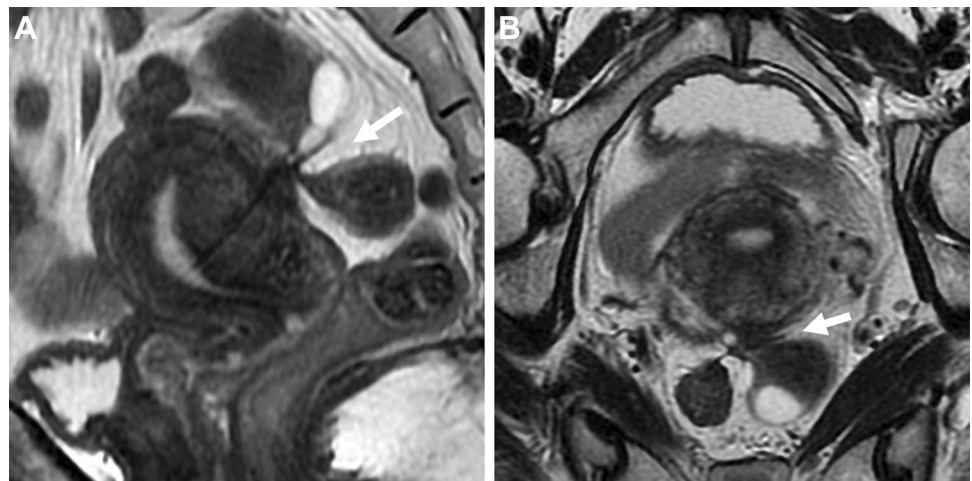
of the ectopic endometrial tissue may cause a variable inflammatory response and fibrous reaction. The endometrial tissue infiltrates the adjacent fibromuscular tissue and induces smooth muscle proliferation and fibrous reaction, resulting in the formation of T2-low signal intensity solid masses as “adenomyosis extern” with irregular, indistinct, or stellate margins, or T2-low signal intensity soft tissue thickening [29–35]. T1-high signal intensity hemorrhagic foci and SWI-signal voids due to hemosiderin deposits may be observed. In one study, 89% of deep endometriosis was revealed on SWI whereas 61% on T1-weighted images [36]. In evaluating posterior cul-de-sac obliteration due to deep endometriosis, retroflexed uterus, elevated posterior vaginal fornix, intestinal tethering and/or a tethered appearance of the rectum in the direction of the uterus, faint strands between the uterus and intestine, and fibrotic plaque and/or



Fig. 2 Endometrioma. A 45-year-old with a history of dysmenorrhea and suspicion of a left ovarian cyst on ultrasonography examination. **A** T2-weighted image reveals a high signal intensity left ovarian cyst (arrow). **B** On fat-saturated T1-weighted image, the left ovarian cyst

(arrow) shows high signal intensity. **C** SWAN reveals dotted to curved linear signal voids in the cyst wall (arrow), which suggest endometrioma

Fig. 3 Deep endometriosis. A 48-year-old with a history of pelvic pain and suspicion of deep posterior endometriosis. **A** Sagittal and **B** oblique coronal T2-weighted images show the elevation of the posterior vaginal fornix, low signal intensity fibrotic plaque with stellate margins (arrow) on the serosal surface of the retroflexed uterus. Tethered appearance of the rectum to the uterus with low signal intensity faint fibrous strands is seen



node covering the serosal surface of the uterus are specific MR findings [37]. In addition, displacement of intraperitoneal fluid is another suggestive finding of posterior cul-de-sac obliteration due to endometriosis [38]. T2-low signal intensity faint strands reflecting fibrotic adhesions should be interpreted with caution in mild cases.

The kissing ovaries sign/cloverleaf sign

Both ovaries may be located close to or are touching each other in the pouch of Douglas referred to as the kissing ovaries sign, usually due to pelvic adhesions (Fig. 4A–D). This finding is strongly related to disease severity and frequency of infertility, and has a significant correlation with deep endometriosis with a sensitivity of 67%, specificity of 68%, and positive predictive value (PPV) of 55% [39]. Occasionally “cloverleaf sign” may be observed: the “leaves” are formed by at least three different organs such as both ovaries,

uterus, or rectum, coming together in the center of the figure formed by constrictive adhesions (Fig. 4E) [40].

Torus uterinus/uterosacral ligament/round ligament

Torus uterinus is anatomically defined by the presence of a small transverse thickening that binds the original insertion of uterosacral ligaments on the posterior wall of the uterus. Torus uterinus and uterosacral ligaments are the most frequent sites of deep endometriosis (86%) [34]. Torus uterinus involvement may appear as a T2-low signal intensity mass or thickening in the upper middle portion of the posterior cervix, and involvement of the uterosacral ligament with endometriosis may bore a nodule with regular or stellate margins or show fibrotic thickening (Fig. 5A–C). Uterosacral ligament involvement may often be asymmetric, unilateral in 40%, and bilateral in 60% [34]. The round ligament involvement is less common (3–5%) with left-side predominance.

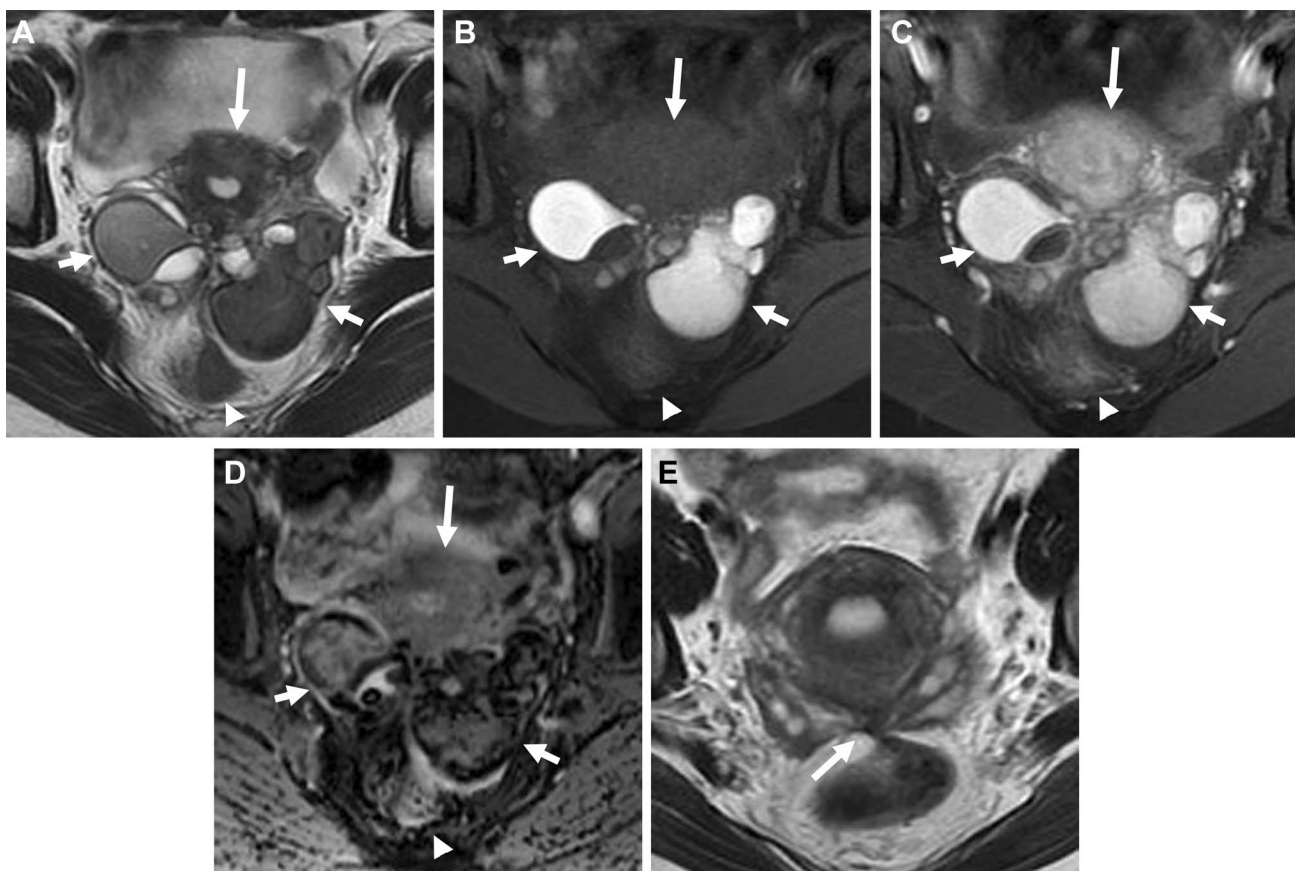


Fig. 4 Deep endometriosis (kissing ovaries /cloverleaf sign). A 27-year-old with a history of irregular menstruation and suspicion of bilateral ovarian cysts on ultrasonography examination. **A** On T2-weighted image and **B** fat-saturated T1-weighted image, bilateral endometriomas (short arrows) are observed posterior to the uterus (long arrow), appearing as “kissing ovaries” with extensive fibrous adhesions exhibit low signal intensity on T2-weighted image and intense contrast enhancement on **C** post-contrast fat-saturated T1-weighted image. A tethered appearance of the rectum (arrowhead)

with T2-low signal intensity faint fibrous strands is observed. Small hemorrhagic foci within deep endometriosis are scattered as T1-high signal intensity spots and spotty signal voids on **D** SWI. Curved linear signal voids along the cyst wall are observed on SWI. A 36-year-old with deep endometriosis shows the cloverleaf sign as both ovaries, uterus, and rectum coming together in the center of the figure formed by low signal intensity constrictive adhesions (arrow) on **E** T2-weighted image

The round ligament is identified as thin structures running from the uterine horns to the pelvic sidewall. The involved ligament may appear thickened, shortened, and irregular, with a nodular appearance (Fig. 5D) [41, 42]. The distal part of the round ligament is situated extra-pelvic site and may appear as a painful, palpable inguinal mass, with menstrual variation in the size or severity of symptoms [43].

Focal adenomyosis located in the outer myometrium (FAOM)

Focal adenomyosis located in the outer myometrium (FAOM) is observed more frequently in women with endometriosis and was significantly associated with deep endometriosis [44–46]. FAOM is separated from the junctional zone which was kept intact and with preserved healthy muscular structures between the adenomyosis and the junctional

zone on T2-weighted images (Fig. 6) [44]. FAOM may be caused by endometriotic invasion from the outside, whereas usual adenomyosis is a product of direct endometrial invasion [44–46].

Urinary tract endometriosis

Urinary tract involvement is rare and occurs in only about 1% of endometriosis. Bladder endometriosis is the most common, and rarely ureteral involvement may occur usually with hydronephroureter. The posterior wall and the dome are commonly affected areas of bladder endometriosis [41, 47, 48]. Less than 30% of patients suffer from cyclical hematuria, because endometrial deposits are usually submucosal and mucosal infiltration is relatively rare. Bladder endometriosis may appear as a T2-low signal intensity solid mass reflecting fibromuscular hyperplasia. T1-high signal

Fig. 5 Deep endometriosis (rectosigmoid/round ligaments). A 29-year-old with a history of dysmenorrhea. **A** T2-weighted image and **B** fat-saturated T1-weighted image reveal a fibrotic plaque (arrow) on the right posterior serosal surface of the uterus to the right uterosacral ligament. Mottled T1-high signal intensity hemorrhagic foci are observed. **C** The right ureter is involved (arrow) resulting in right hydronephrosis on coronal T2-weighted image. A 46-year-old with right endometrioma. **D** On T2-weighted image, the right thickened round ligament (arrow) and a tethered appearance of the rectum to the uterus with low signal intensity faint fibrous strands (arrowhead) are revealed

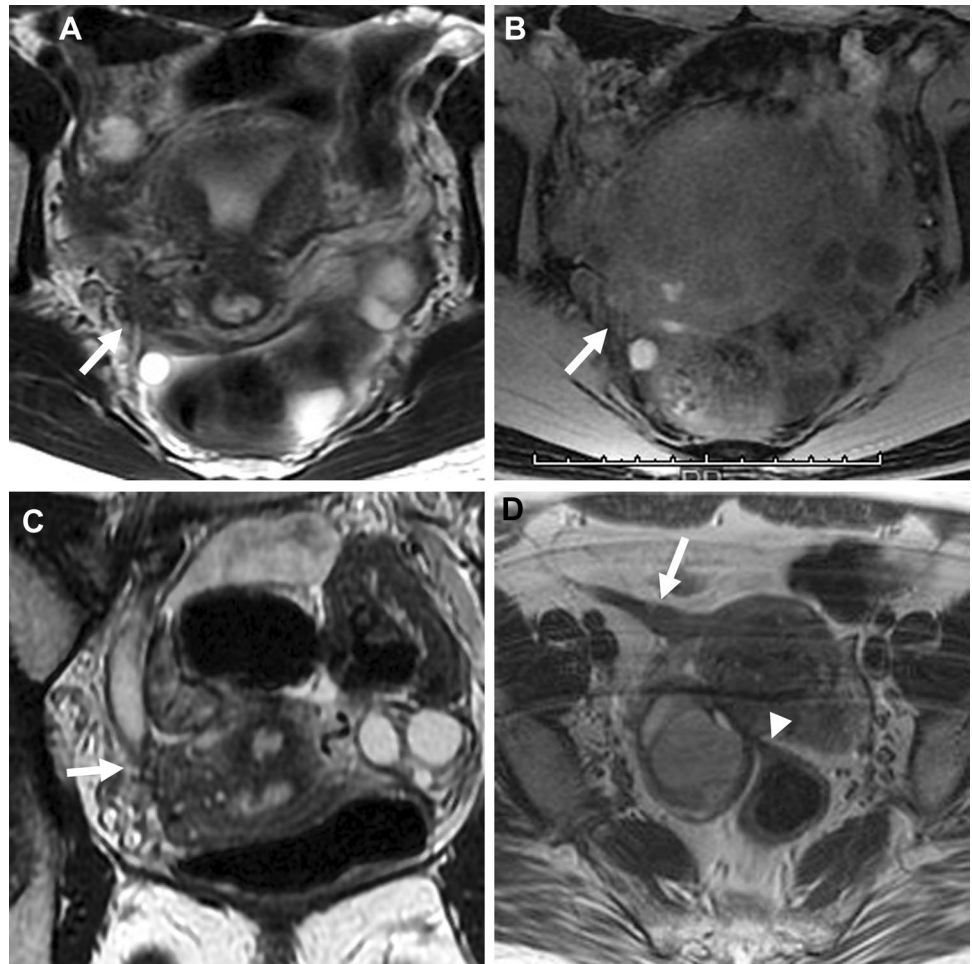
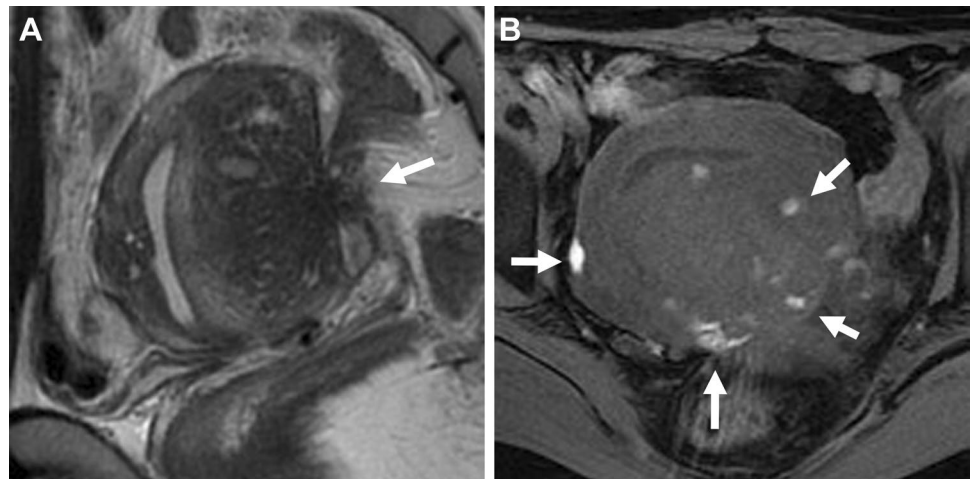


Fig. 6 Focal adenomyosis located in the outer myometrium (FAOM). A 39-year-old with a history of dysmenorrhea and hypermenorrhea. **A** On sagittal T2-weighted image ill-defined low signal intensity area is revealed in the thickened posterior myometrium separated from the junctional zone. Low signal intensity fibrous plaque with adhesive change (arrow) is seen posterior to the myometrial lesion. **B** On fat-saturated T1-weighted image high signal intensity hemorrhagic spots (arrows) are scattered



intensity small hemorrhagic foci may be observed within the mass (Fig. 7) [47]. Signal voids due to hemosiderin deposits reflecting repeated cyclic hemorrhage on SWI are characteristic, and more sensitive than T1-weighted images [49].

Extra-peritoneal involvement of endometriosis may cause adhesive stricture of the ureter resulting in

hydronephroureter. Preoperative diagnosis may be often difficult because it may occur with no obvious mass formation, and thin slice T2-weighted images can reveal low signal intensity fibrous adhesion [41, 48]. DWI could differentiate endometriosis-related hydronephroureter from ureteral cancer. Cancer appears as a DWI-high signal intensity lesion,

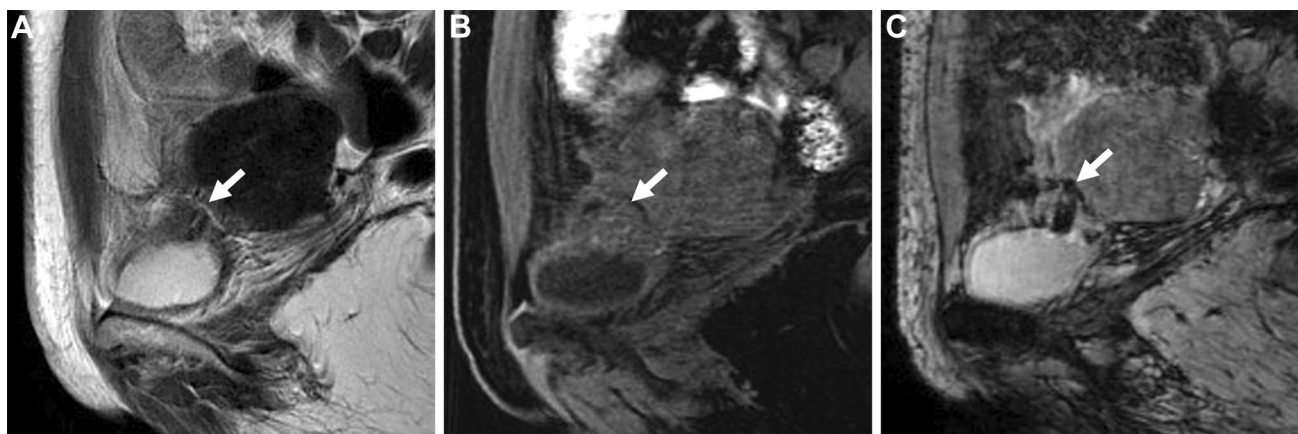


Fig. 7 Bladder endometriosis. A 42-year-old with frequent urination during menstruation. **A** Sagittal T2-weighted image shows low signal intensity mass (arrow) at the posterior wall of the bladder. Small

hemorrhagic foci are scattered in the mass (arrow) as high signal intensity spots on **B** sagittal fat-saturated T1-weighted image and dotted signal voids on **C** sagittal SWAN

whereas endometriosis does not cause a signal increase on DWI.

Bowel endometriosis

Rectosigmoid (65.7%) is the most common site of deep endometriosis involving bowels, followed by ileocecal junction (20%) and rectum (15%). Endometrial implants adhere to the bowel serosa and invade the muscle layers with marked smooth muscle proliferation, consequently, irregular bowel wall thickening with stricture formation resembling carcinoma. No mucosal involvement is a helpful finding to differentiate from cancer on barium enema or colonoscopy [41, 50–52]. The involved bowel wall may appear as a T2-low signal intensity mass reflecting fibromuscular

hyperplasia with small hemorrhagic foci revealed as T1-high signal intensity spots and/or SWI-signal voids (Fig. 8) [49, 50]. "Mushroom cap" shaped appearance is characteristic of rectosigmoid endometriosis: heterogeneous T2-low signal intensity hypertrophic muscularis propria, covered with T2-high signal intensity mucosa and submucosa (Fig. 8A) [51].

Retroperitoneal endometriosis (lymph node involvement)

Pelvic endometriosis may often involve adjacent retroperitoneal space, however, extra-pelvic retroperitoneal endometriosis is rare. The pathogenesis is thought to be secondary to retrograde menstruation, vascular or

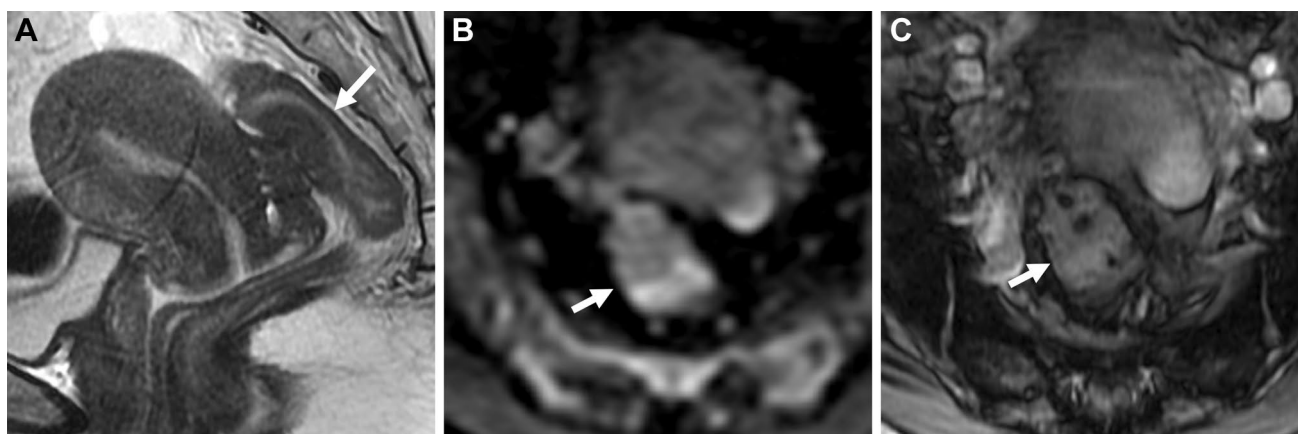


Fig. 8 Bowel endometriosis. A 47-year-old with hematochezia during menstruation. **A** On sagittal T2-weighted image, the anterior wall of the rectosigmoid colon is thickened exhibiting low signal intensity covered by high signal intensity mucosa and submucosa as "mushroom cap" shaped appearance (arrow). Low signal intensity fibrous

strands between the uterus and rectosigmoid colon are observed. **B** DWI ($b=800 \text{ s/mm}^2$), **C** SWAN. The mass-like thickened wall (arrow) shows no diffusion restriction on DWI. Small hemorrhagic foci are scattered as dotted signal voids on SWAN

lymphatic spread, or coelomic metaplasia, and lymphatic spread is the most possible cause. Occasionally retroperitoneal lymph nodes contain endometrial tissue (Fig. 9) [41, 53, 54].

Abdominal wall/subcutaneous endometriosis

Abdominal wall endometriosis usually develops in association with previous surgical scars such as cesarean section, but spontaneous abdominal involvement may also occur. Cyclic abdominal discomfort or pain with a palpable mass may suggest abdominal wall endometriosis. Inhomogeneous signal intensity mass on T2-weighted images due to the admixture of fibrosis, hemorrhage, and endometrial tissue, T1-high signal intensity spotty hemorrhage, and SWI-signal voids due to hemosiderin deposits are helpful for the diagnosis (Fig. 10) [41, 49, 55–58]. Linear infiltration irradiating peripherally from a central soft tissue nodule as the gorgon sign is suggestive CT finding (Fig. 10E) [55]. Subcutaneous endometriosis may occasionally appear as an endometrioma-like hemorrhagic cystic mass.

Thoracic endometriosis

Thoracic endometriosis is rare, and classified as either pleural (Fig. 11A) or parenchymal endometriosis (Fig. 11B) [41, 59–61]. Patients with pleural endometriosis may complain of chest pain and dyspnea due to catamenial pneumothorax (70%) or hemothorax, whereas patients with parenchymal endometriosis usually complain of hemoptysis in the menstrual phase. Pleural endometriosis may appear as T1-high signal intensity nodules at the diaphragm and may be located mostly on the right side and posterior to the vena cava [59]. Pulmonary lesions may appear as patchy ground-glass opacities on CT due to hemorrhage which vary in size during

the menstrual cycle and may disappear after the cessation of menstruation.

Complications

Ruptured endometrioma

Rupture of endometrioma may occur in 3% of cases, and cause acute chemical peritonitis with severe abdominal pain. Ruptured endometrioma with the absence of tense, flabby, or depressed surface, and hemorrhagic fluid collection in the peritoneal cavity may show T1-high signal intensity clarified on fat-saturated T1-weighted images (Fig. 12A, B) [62, 63]. Strong peritoneal enhancement may be observed on contrast-enhanced images reflecting chemical peritonitis (Fig. 12C).

Torsion of endometrioma

Torsion of the endometrioma is less common than those of other adnexal masses, possibly due to surrounding adhesions [63]. Patients present acute, intermittent lower abdominal pain. Lack of contrast enhancement of the cyst wall suggests complete torsion of endometrioma.

Pelvic inflammatory disease

Pelvic inflammatory disease (PID) may be complicated with endometriomas. Infected endometrioma may have thickened walls reflecting fibrous capsules with inflammatory granulation tissue. Usually, tubo-ovarian abscess contains T1-low, T2-high, and DWI-high signal intensity pus, and the admixture of T1-high signal intensity hemorrhagic contents may be suggestive of infected endometrioma [64, 65].

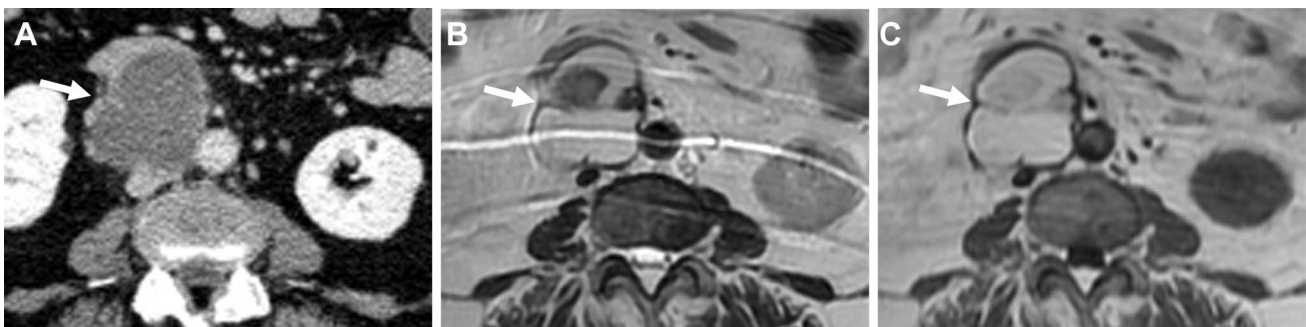


Fig. 9 Retroperitoneal endometriosis (lymph node involvement). A 72-year-old with suspicion of abdominal mass on ultrasonography examination. **A** Contrast-enhanced CT reveals a cystic mass (arrow)

located in the retroperitoneal space. The mass shows high signal intensity on both **B** T2-weighted image and **C** T1-weighted image suggesting its hemorrhagic contents with clots

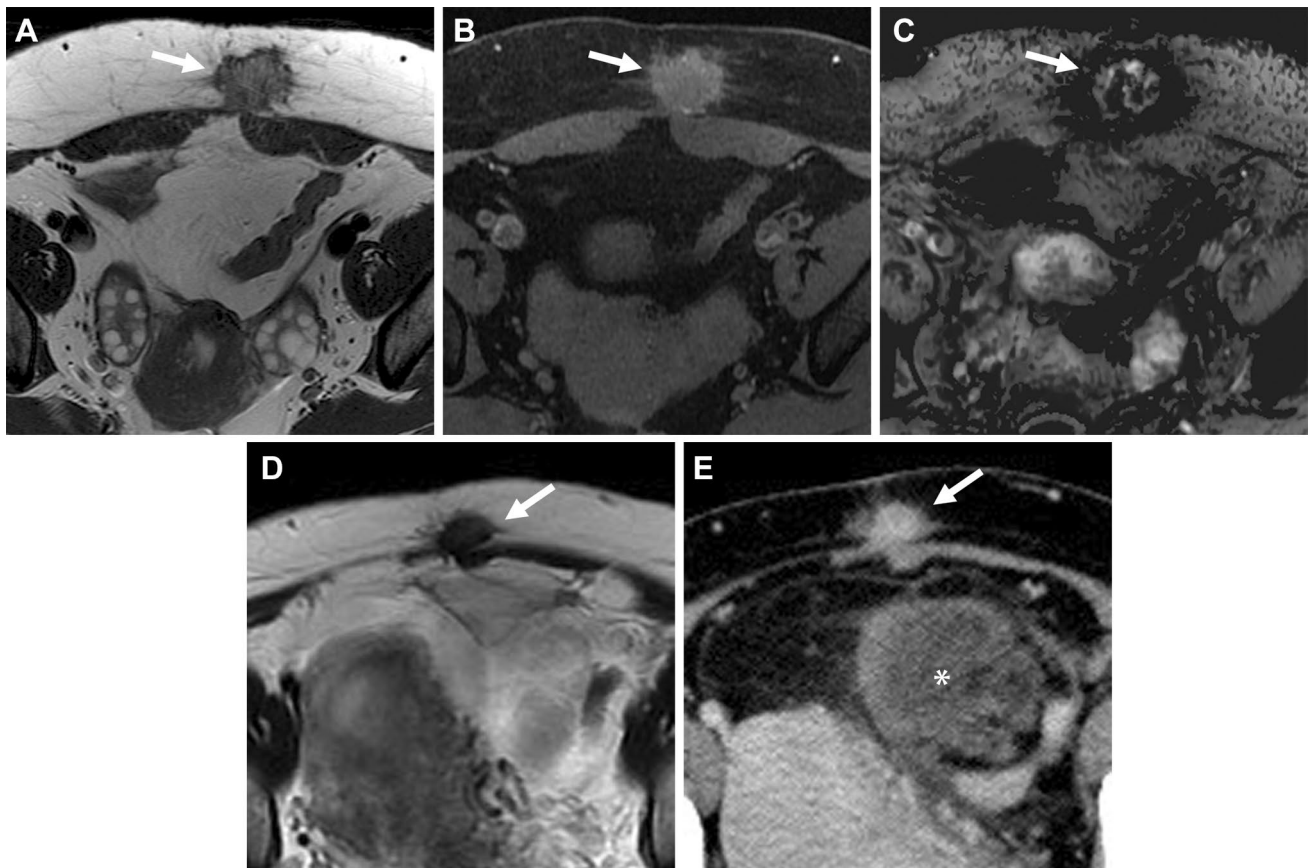
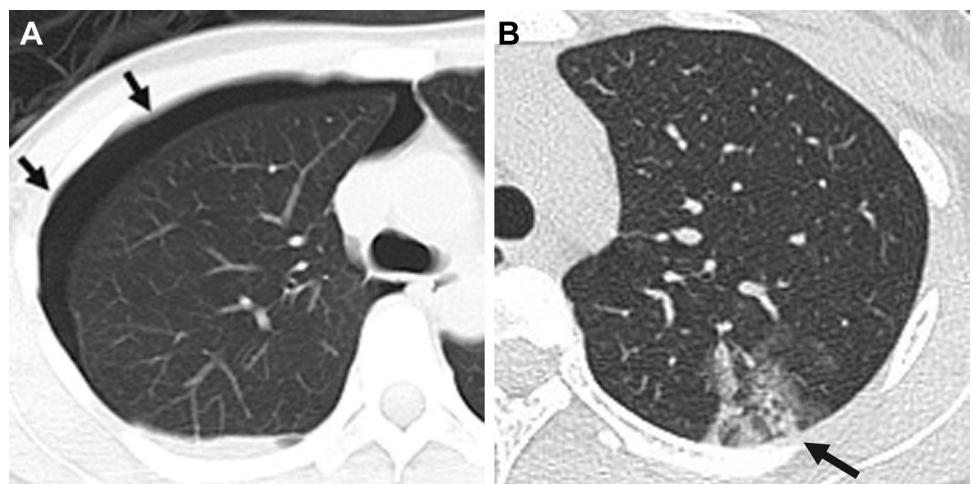


Fig. 10 Abdominal wall endometriosis. A 34-year-old with lower abdominal discomfort during menstruation. **A** On T2-weighted image, a subcutaneous mass with irregular margins (arrow) exhibits heterogeneous signal intensity at the previous cesarean surgical scar. Small high signal intensity hemorrhagic foci are revealed on **B** fat-saturated T1-weighted image. Prominent signal voids are observed

in and around the mass (arrow) on **C** SWI. A 37-year-old with lower abdominal discomfort during menstruation. **D** On T2-weighted image a subcutaneous low signal intensity mass (arrow) at the previous cesarean surgical scar is revealed. **E** On CT, linear infiltration irradiating peripherally from a central soft tissue mass (arrow) as the gorgon sign is observed. *: Concomitant mesenteric liposarcoma

Fig. 11 Thoracic endometriosis. A 36-year-old with repeated catamenial right pneumothorax. **A** On CT, right pneumothorax (arrows) is observed. A 28-year-old with repeated catamenial hemoptysis. **B** On CT, patchy ground-glass opacity (arrow) at the left upper lobe reflecting pulmonary hemorrhage is observed



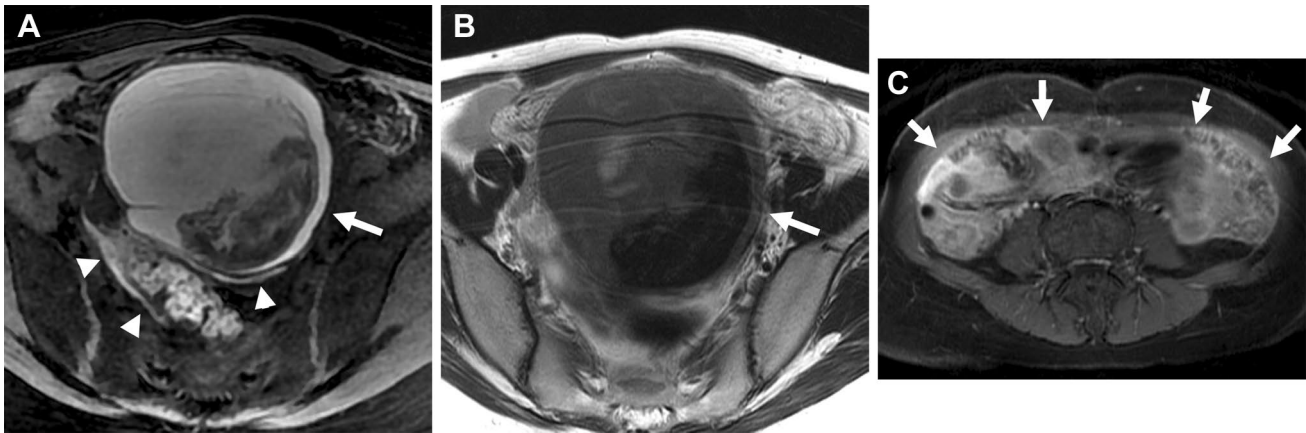


Fig. 12 Ruptured endometrioma. A 26-year-old with acute abdomen. MRI is obtained at 3 days after the onset. **A** Fat-saturated T1-weighted image and **B** T2-weighted image show a left endometrioma (arrow) with a lack of tension. High signal intensity peritoneal

fluid collection (arrowheads) is revealed on fat-saturated T1-weighted image. Diffuse intense contrast enhancement (arrows) is observed on **C** the post-contrast fat-saturated T1-weighted image reflecting chemical peritonitis

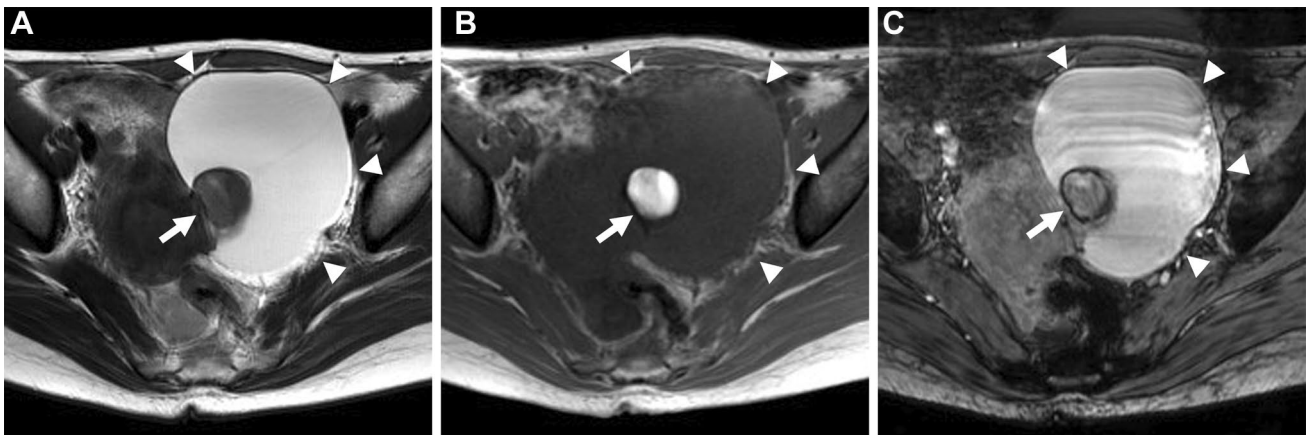


Fig. 13 Peritoneal inclusion cyst associated with endometriosis. A 32-year-old with suspicion of a large ovarian cyst on ultrasonography examination. **A** T2-weighted image and, **B** T1-weighted image show a left small endometrioma (arrow) surrounded by a pseudocystic fluid

collection (arrowheads) defined by the pelvic wall and pelvic organs. **C** SWAN revealed curved linear signal voids along the wall of the endometrioma

Peritoneal inclusion cyst

Peritoneal inclusion cysts are localized fluid collection observed in the adhesive pelvis after surgical procedures, trauma, inflammation, or endometriosis. Extensive pelvic adhesions may trap the intraperitoneal fluid and form the pseudocystic lesion. Peritoneal inclusion cyst may appear as a cystic lesion with an irregular margin defined by the adjacent pelvic structures on imaging (Fig. 13) [66].

Malignant transformation

Endometriomas are associated with a risk of malignant transformation (1% of cases) [67–69]. Endometriosis-associated ovarian carcinoma (EAOC) affects 40–50 years, it is 10–20 year younger than ovarian cancer without endometriosis [67]. Because estrogen may have a role in malignant transformation, patients of reproductive age should be treated, or followed closely. Endometrioma is the precursor lesion for carcinomas via atypical endometriomas through

pathways related to oxidative stress, inflammation, and hyperestrogenism and finally to genomic alterations [67, 70]. Persistent oxidative stress induced by endometriosis-dependent hemorrhage may be associated with carcinogenesis [71]. The most frequent histological types of EAO are endometrioid and clear cell carcinomas [67, 72]. Gene mutation analyses identified oncogenic mutations in endometriosis and normal endometrium and revealed that the same mutations were present in different endometriotic lesions. EAO may be caused by eutopic endometrial glandular epithelial cells with oncogenic mutations that have undergone menstrual blood reflux and engrafted in the ovary, rather than by low-risk endometriosis acquiring oncogenic mutations and becoming malignant [67, 73].

There are three major pathways for the development of endometriosis-related ovarian neoplasm (ERON). The most major pathway is epithelial malignancies (EAO) arising by step-wise carcinogenesis, with endometrioid and clear cell

carcinomas which are the representative histologic types. Endometrial cells with genetic mutations retrogradely reach the ovary with endometrioma and become cancers promoted by the internal environment of endometrioma. Estrogen receptor-positive cells become endometrioid carcinomas via atypical endometriosis with estrogen stimulation, sometimes occurring bilaterally or with endometrioid carcinoma of the uterine endometrium. On the other hand, estrogen receptor-negative cells become clear cell carcinomas promoted by iron oxidative stress caused by hemorrhagic products in endometriomas and are usually unilateral [70, 74, 75]. The other pathways include other Müllerian-type tumors (seromucinous borderline tumor and mesonephric-like adenocarcinoma) and sarcomas (adenosarcoma, carcinosarcoma, and endometrioid stromal sarcoma). These pathways are rare, and the pathogenesis of endometriosis-associated other Müllerian-type tumors and sarcomas is not well established.

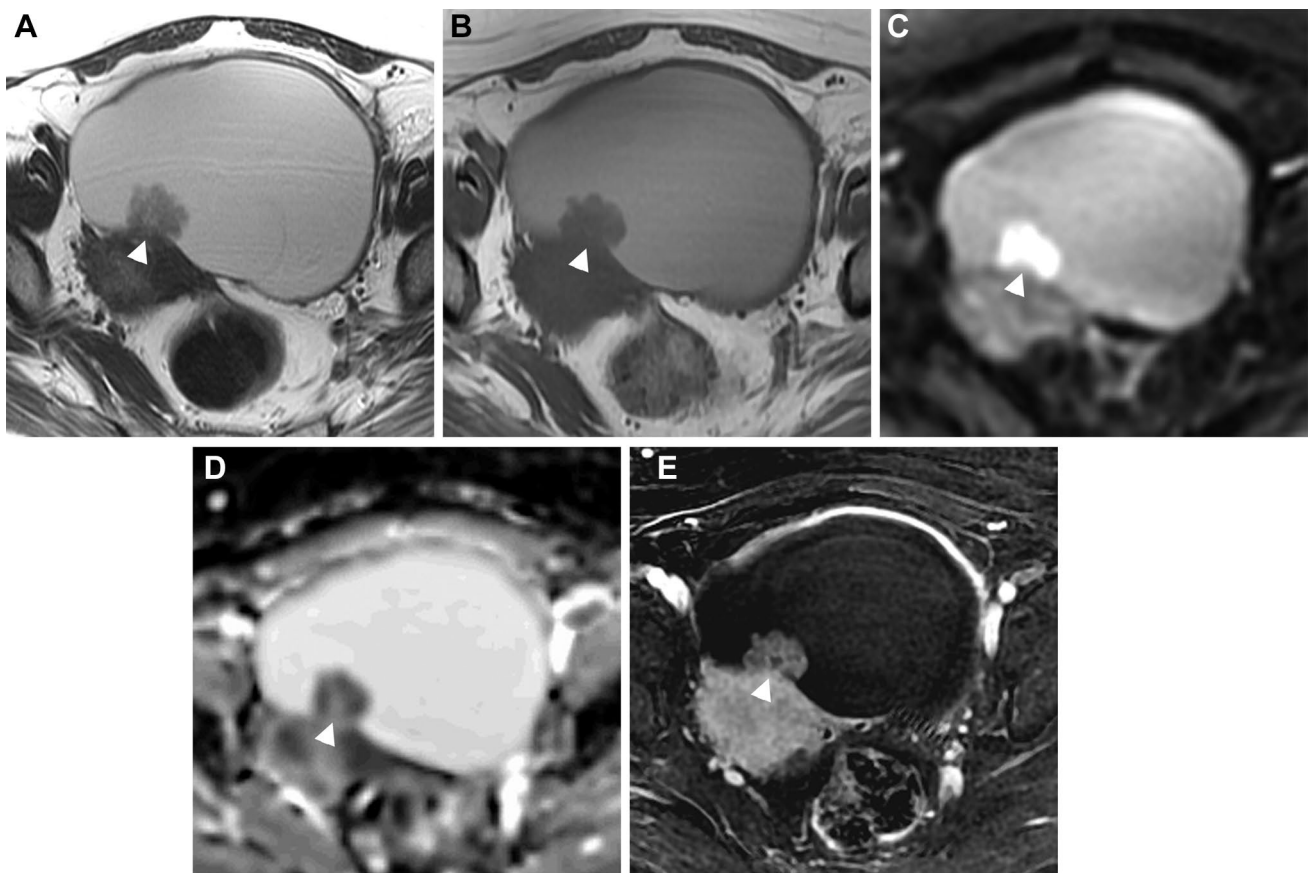


Fig. 14 Endometriosis-associated ovarian carcinoma: clear cell carcinoma. A 52-year-old with suspicion of an ovarian cystic mass with mural nodules on ultrasonography examination. **A** T2-weighted image, **B** T1-weighted image, **C** DWI ($b=800 \text{ s/mm}^2$), **D** ADC map, and **E** contrast-enhanced subtraction image show a left ovarian cystic mass with a mural nodule (arrowhead). The cyst contents show high

signal intensity on both T1- and T2-weighted images reflecting hemorrhagic fluid. The mural nodule shows intermediate signal intensity on T2-weighted image and water diffusion restriction on DWI, and intense contrast-enhancement on post-contrast images clarified on the subtraction image

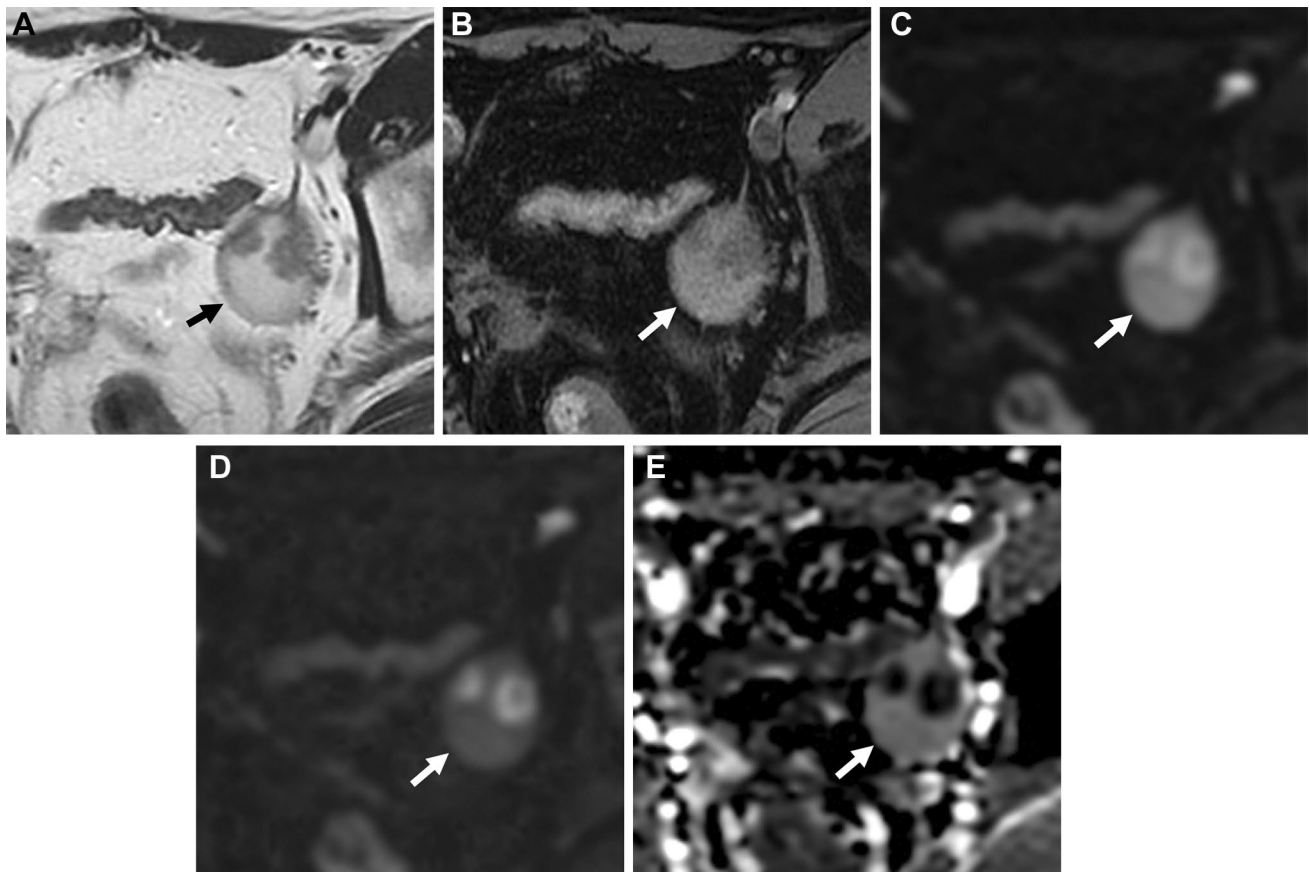


Fig. 15 Endometriosis-associated ovarian carcinoma: endometrioid carcinoma. A 35-year-old with suspicion of an ovarian cystic mass with mural nodules on ultrasonography examination. **A** T2-weighted image, **B** fat-saturated T1-weighted image, **C** DWI ($b=800 \text{ s/mm}^2$), **D** computed DWI with high b value ($b=1500 \text{ s/mm}^2$), and **E** ADC map show a left ovarian cystic mass (arrow) with mural nodules. The

cyst contents show high signal intensity on both T1- and T2-weighted images reflecting hemorrhagic fluid. The mural nodules show water diffusion restriction on DWI, however, high signal intensity hemorrhagic cyst contents mask the signal of mural nodules. High b -value computed DWI can reduce the signal of cyst contents and high signal intensity of mural nodules is clarified

Imaging criteria of malignant transformation

A definite MR finding of malignant transformation is the appearance of contrast-enhanced mural nodules in endometriomas. The contrast-enhancement of the mural nodule may be masked by T1-high signal intensity hemorrhagic fluid, and could be well visualized on contrast-enhancement subtraction images [67, 76, 77]. However, small benign mural nodules may occasionally show contrast enhancement [78]. The malignant mural nodule shows T2-intermediate and DWI-high signal intensities with low apparent diffusion coefficient (ADC) reflecting hypercellularity (Figs. 14, 15), however, clots in the endometrioma may also show DWI-high signal intensity with low ADC mimicking malignant mural nodules (Fig. 16) [79]. The absence of contrast-enhancement of the clots is diagnostic, however, it may be not always clear due to surrounding T1-high signal intensity hemorrhagic fluid. Contrast-enhancement subtraction

images are critical for the differentiation by revealing no contrast-enhancement of the clots (Fig. 16C) [77]. SWI may help distinguish the clots, which show low signal intensity reflecting blood products from malignant mural nodules without using contrast materials (Fig. 16F). DWI of hemorrhagic cyst contents in the endometrioma may show high signal intensity, making it difficult to evaluate the signal of mural nodules. High b value ($\geq 1500 \text{ s/mm}^2$) computed DWI may be useful for evaluating high signal intensity malignant mural nodules with reduced signal in the cyst contents (Figs. 15, 17).

The disappearance of T2-"shading" and T1-signal decrease due to the dilution by tumor secretion is a suggestive finding of malignant transformation. Other suggestive features of malignant transformation include interval enlargement of the endometrioma and spontaneous reduction in dysmenorrhea due to the reduction of functional endometrial tissue replaced by tumoral tissue [67, 78, 80, 81].

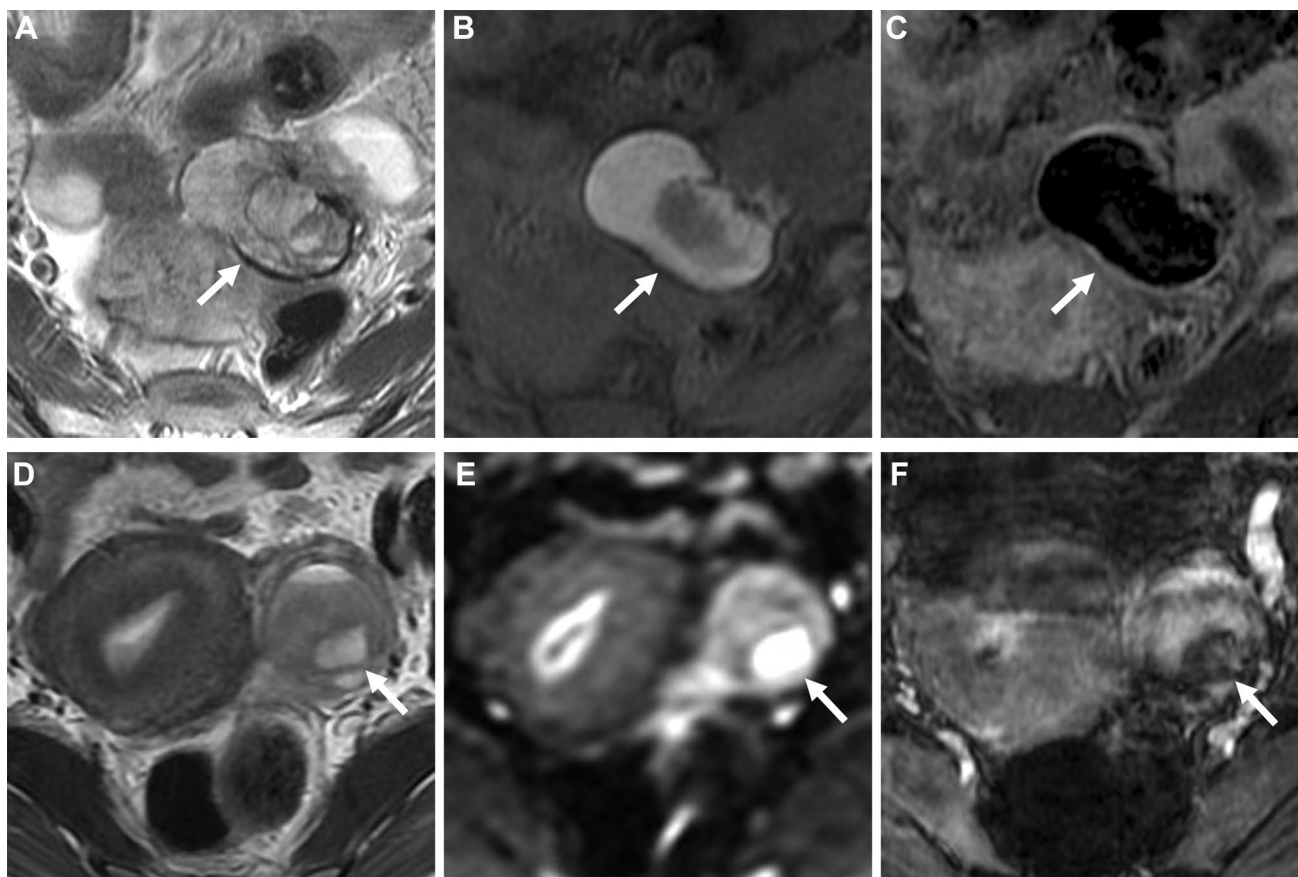


Fig. 16 Clots in endometrioma. A 34-year-old with suspicion of an ovarian cystic mass with mural nodules on ultrasonography examination. **A** T2-weighted image, **B** fat-saturated T1-weighted image, and **C** contrast-enhanced subtraction image show a left endometrioma (arrow) with a solid component. The solid component shows intermediate signal intensity on T2-weighted image. The high signal intensity of cyst contents masks the signal of the solid component on the post-

contrast image, and no contrast enhancement of the clot is revealed on the contrast-enhanced subtraction image. A 27-year-old with a history of dysmenorrhea. **D** T2-weighted image, and **E** DWI ($b=800 \text{ s/mm}^2$) show a left endometrioma (arrow) with a solid component. The solid component shows intermediate signal intensity on T2-weighted image and water diffusion restriction on DWI, however, appears as a signal void on **F** SWAN suggesting a clot

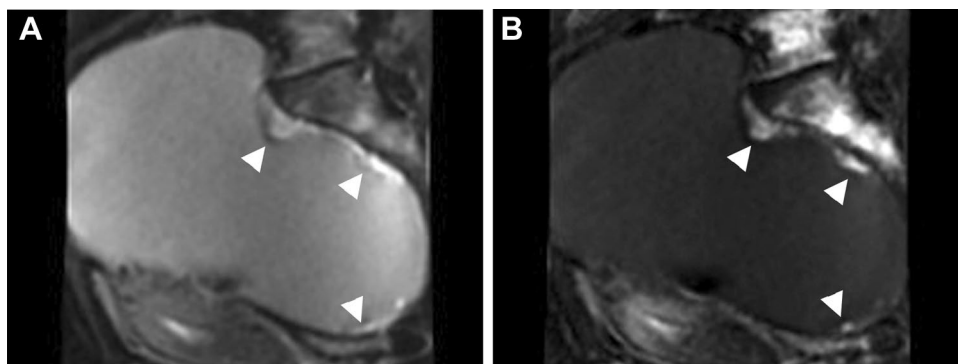


Fig. 17 Endometriosis-associated ovarian carcinoma: clear cell carcinoma. A 47-year-old with suspicion of an ovarian cystic mass with mural nodules on ultrasonography examination. **A** On sagittal DWI (reduced field-of-view DWI, $b=800 \text{ s/mm}^2$) a large left endome-

trioma with small mural nodules (arrowheads) is observed. The high signal intensity of the cyst contents masks the signal of small mural nodules and **B** computed DWI ($b=2000\text{s/mm}^2$) clarified the high signal intensities of the small mural nodules (arrowheads)

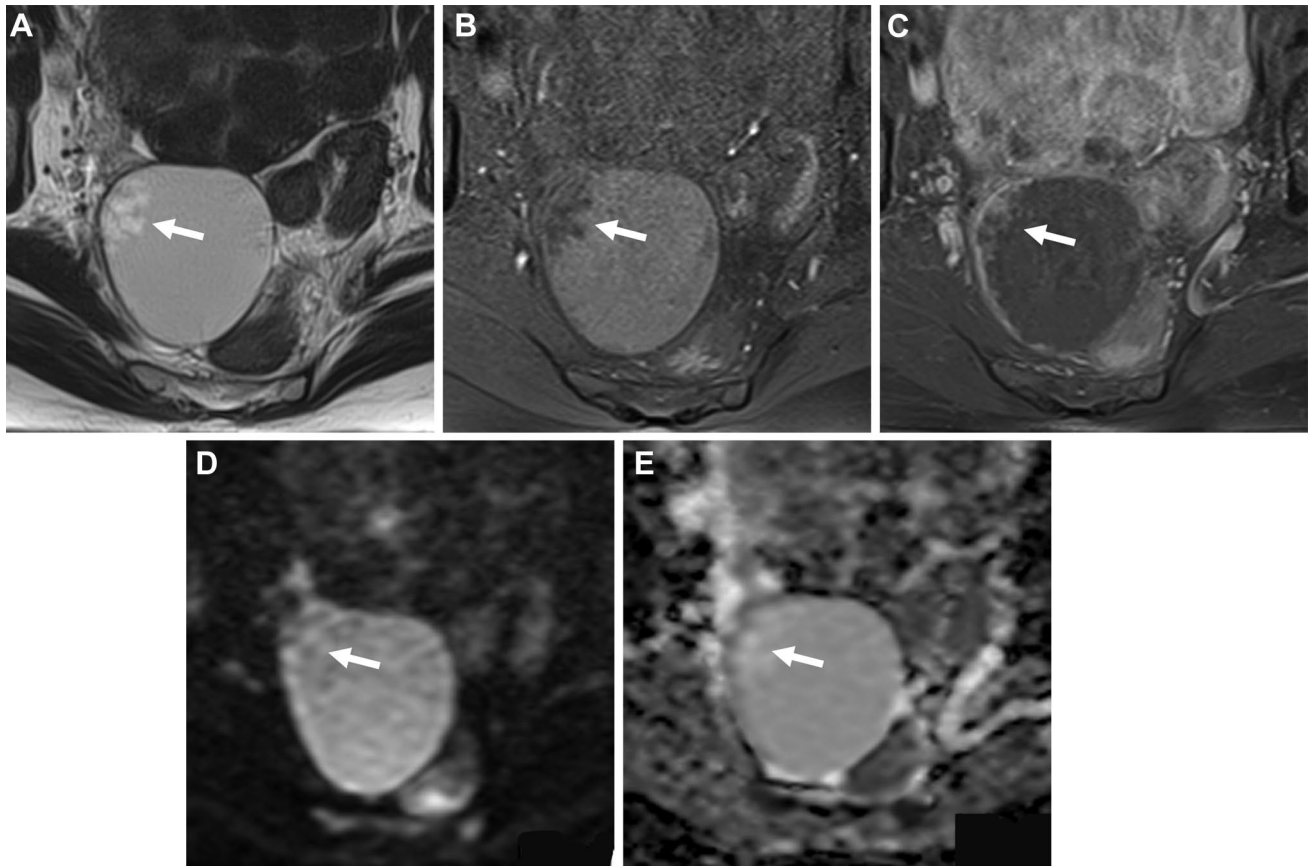


Fig. 18 Endometriosis-related ovarian neoplasm: seromucinous borderline tumor. A 55-year-old with suspicion of an ovarian cystic mass with mural nodules on ultrasonography examination. **A** T2-weighted image, **B** fat-saturated T1-weighted image, **C** contrast-enhanced subtraction image, **D** DWI ($b = 800 \text{ s/mm}^2$), **E** ADC map show an endo-

metrioma with a papillary mural nodule (arrow). The papillary mural nodule shows high signal intensity with low signal intensity dendritic fibrous core on T2-weighted image, relatively weak contrast-enhancement, and high signal intensity on DWI with high ADC (T2 shine-through)

Seromucinous borderline tumor

Seromucinous borderline tumor (SMBT) is an uncommon Müllerian-type tumor arising in endometriomas (at least 1/3 cases). SMBT may affect relatively younger patients (30–40's) and fertility-preserving surgery may be considered. SMBT may appear as papillary mural nodules within the endometrioma exhibiting T2-high signal intensity, weak contrast-enhancement, and DWI-high signal intensity with high ADC due to T2 shine-through effects reflecting edematous stroma with abundant mucinous material. The mural nodules may contain T2-low signal intensity dendritic fibrous core (Fig. 18) [82–84].

Mesonephric-like adenocarcinoma

Mesonephric-like adenocarcinoma is a rare Müllerian-type tumor arising in the uterine corpus and ovaries. Histologic and immunohistochemical features overlap with those of

cervical mesonephric adenocarcinoma. Mesonephric-like adenocarcinoma may arise from endometriosis as ERON, and affects mostly postmenopausal patients with aggressive behavior [85, 86].

Sarcomas

Carcinosarcoma is a rare ovarian tumor (2% of ovarian malignancies), which is a biphasic neoplasm composed of high-grade malignant epithelial and mesenchymal elements. Carcinosarcoma may arise from endometriosis, mostly with endometrioid carcinoma, and exhibit as a large mass with stained-glass appearance, hemorrhage, and necrosis on MRI [87]. Adenosarcoma is a rare neoplasm of low-grade malignancy that consists of an admixture of sarcomatous mesenchymal and benign glandular epithelial components. It arises most commonly in the uterine endometrium, but may also occur in the ovaries, and extragenital sites in association with endometriosis [88]. Endometrial stromal sarcoma is a

rare malignant uterine tumor originating from endometrial stromal cells. Endometrioid stromal sarcoma may originate primarily from extra-uterine sites such as the ovaries, peritoneal cavity, retroperitoneum, and vagina associated with endometriosis [89].

Clear cell carcinoma via adenofibroma

Ovarian cancer may arise from benign adenomas or adenofibromas as step-wise carcinogenesis. Especially, a solid variant of clear cell carcinoma (CCC) may arise from non-cystic endometriosis via clear cell adenofibroma (CCAF) as the CCAF–CCC sequence [90, 91]. Clear cell adenofibroma components co-exist in 15–21% of clear cell carcinomas and show lower tumor grade and better prognosis. The malignant focus of clear cell carcinoma arising from clear cell adenofibroma shows DWI-high signal intensity with low ADC and intense early and prolonged contrast enhancement [92].

Endometriosis-associated tumor-like lesions

Decidualized endometrioma during pregnancy

With the hypertrophy of the endometrial stromal cells, the normal uterine endometrium may thicken and transform into the decidua induced by progesterone during pregnancy. This phenomenon may also occur in ectopic endometrial tissue such as endometrioma. Decidualized endometrioma may manifest as broad-based, flat or polypoid mural nodules with smooth contours. Signal intensity is similar to that of the placenta: T2-prominent high signal intensity and DWI-high signal intensity with high ADC (T2 shine-through) reflecting edematous, vascularized decidualized tissue. The ADC measurement is useful for differentiating decidualized nodules from malignant transformation (Fig. 19) [93, 94]. Computed DWI with high b values ($b \geq 1500$ s/mm²) can distinguish decidualized endometriomas from ovarian cancers by visual evaluation.

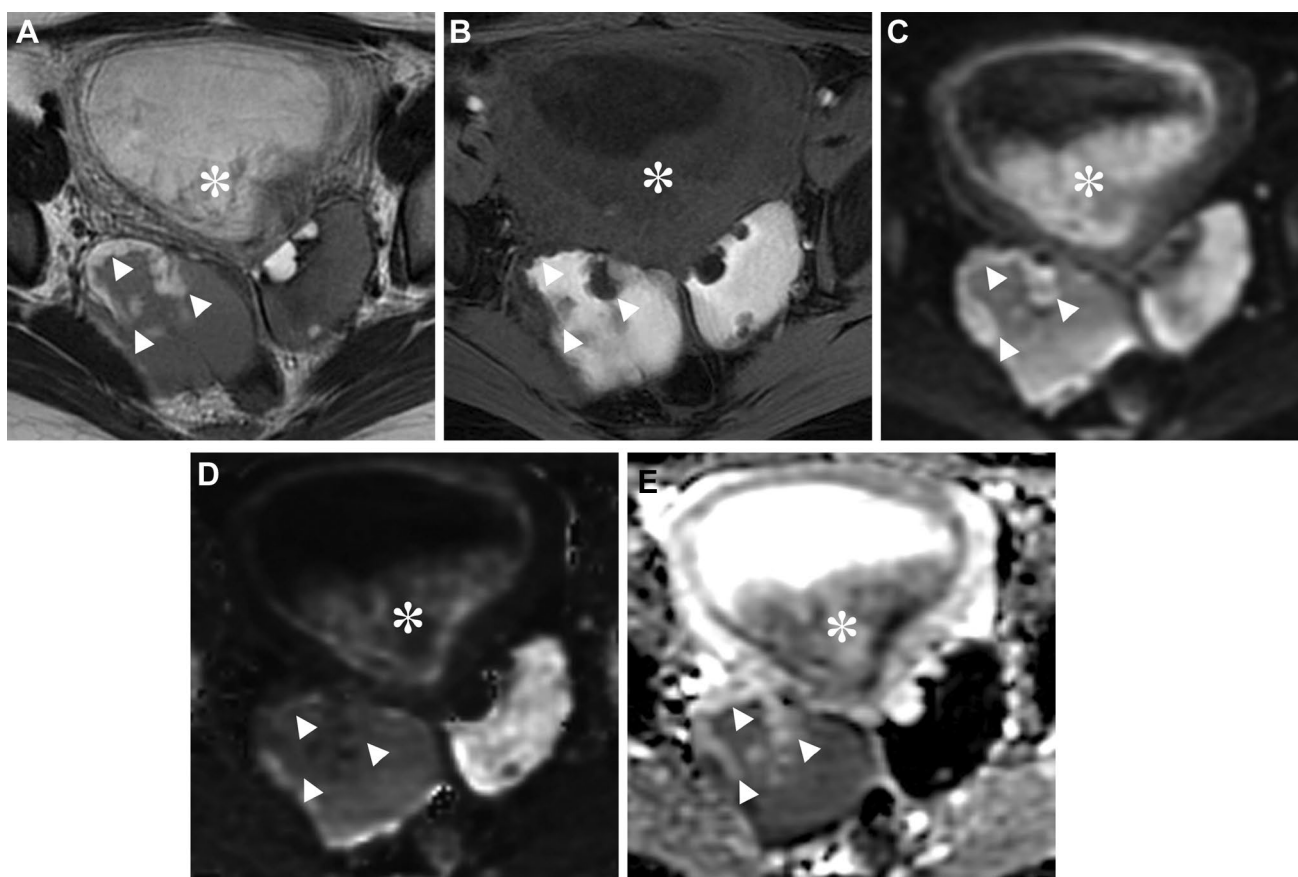
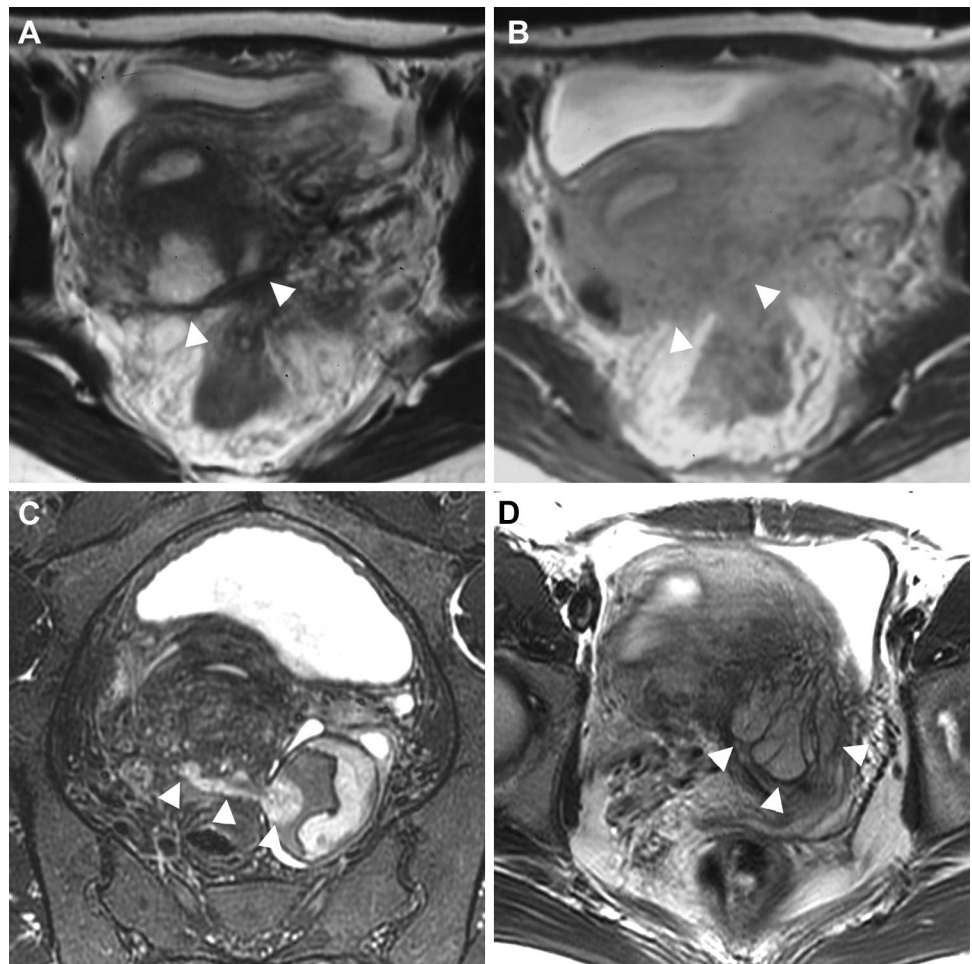


Fig. 19 Decidualized endometrioma. A 32-year-old pregnant (13 weeks) with suspicion of an ovarian cystic mass with mural nodules on ultrasonography examination. A T2-weighted image, B fat-saturated T1-weight image, C DWI ($b=800$ s/mm²). D computed DWI ($b=2000$ s/mm²), and E ADC map show a right endometrioma

with multiple, flat mural nodules (arrowheads) exhibiting T2-prominent high signal intensity, T1-low signal intensity, and high signal intensity on DWI with high ADC (T2 shine-through) similar to those of the placenta (*). On the high b -value ($b=2000$ s/mm²) computed DWI shows the signal decrease of the mural nodules

Fig. 20 Polypoid endometriosis. A 47-year-old with lower abdominal pain associated with genital bleeding and suspicion of deep endometriosis. **A** T2-weighted image and **B** post-contrast T1-weighted image show polypoid masses (arrowheads) exhibiting T2-high signal intensity and intense contrast-enhancement protruding to the posterior wall of the uterine body with adenomyosis. The masses are surrounded by T2-low signal intensity adhesive fibrous tissue as “black rim sign”. The fibrous rim also shows intense contrast enhancement. A 33-year-old with a history of hypermenorrhea and dysmenorrhea and suspicion of deep endometriosis. **C**. Oblique coronal fat-saturated T2-weighted image shows a left endometrioma with high signal intensity mural nodule that extends to the Douglas’ pouch (arrowheads). A 30-year-old with a history of dysmenorrhea and suspicion of deep endometriosis. **D** T2-weighted image shows polypoid masses infiltrating into the myometrium (arrowheads)



Decidualized mural nodules show signal decrease on computed DWI with high b values (Fig. 19D), whereas high signal of malignant mural nodules is maintained [95].

Because both decidualized endometrioma and SMBT may appear as T2-high signal intensity mural nodules in the endometriomas, differentiation becomes problematic if the tumor is detected during pregnancy. Both lesions show DWI-high signal intensity with high ADC (T2 shine-through), and morphological appearances may be the clues for the differential diagnosis. The greater number and lower height are suggestive of decidualized endometrioma, whereas the lobulated margin, pedunculated configuration, and T2-low signal intensity core (the reported frequency ranges from 43 to 61%) of mural nodules are suggestive of SMBT [84, 96].

Polypoid endometriosis

Polypoid endometriosis is a rare variant of endometriosis with histological features resembling those of endometrial polyps. Polypoid endometriosis frequently affects perimenopausal women and hormonal factors such as unopposed

estrogen therapy or tamoxifen use may play a role in its pathogenesis and forms large, often multiple polypoid masses simulating malignancy [97]. Polypoid endometriosis may arise within the endometrioma mimicking malignant transformation, or exist in the pelvic cavity protruding to adjacent structures simulating peritoneal carcinomatosis. The edematous endometriotic tissue may show T2-high signal intensity and DWI-high signal intensity with high ADC (T2 shine-through), and intense contrast enhancement like an endometrial polyp (Fig. 20) [98]. Characteristic surrounding T2-low signal intensity adhesive fibrous tissue in the peritoneal lesions as “black rim” sign suggests its deep endometriosis origin (Fig. 20A) [98, 99]. Polypoid endometriosis may often show areas of hyperplasia and rarely cause malignant transformation, which is usually, endometrioid carcinoma. A reported case of peritoneal polypoid endometriosis with malignant transformation showed T2-high signal intensity and weak contrast enhancement similar to the signal pattern of well-differentiated endometrial carcinoma of the uterus [100].

Conclusions

In evaluating the severity and location of the endometriosis (endometrioma, deep endometriosis, and extra-genital endometriosis), and for the diagnosis of various complications of endometriosis, malignant transformation, and endometriosis-related tumor-like lesions MRI including advanced MR techniques is a non-invasive tool that is feasible for the diagnostic strategy by its good tissue contrast and multiplanar capability.

Open Access This article is licensed under a Creative Commons Attribution 4.0 International License, which permits use, sharing, adaptation, distribution and reproduction in any medium or format, as long as you give appropriate credit to the original author(s) and the source, provide a link to the Creative Commons licence, and indicate if changes were made. The images or other third party material in this article are included in the article's Creative Commons licence, unless indicated otherwise in a credit line to the material. If material is not included in the article's Creative Commons licence and your intended use is not permitted by statutory regulation or exceeds the permitted use, you will need to obtain permission directly from the copyright holder. To view a copy of this licence, visit <http://creativecommons.org/licenses/by/4.0/>.

References

- Zondervan KT, Becker CM, Missmer SA. Endometriosis. *N Engl J Med*. 2020;26(382):1244–56.
- Shafirir AL, Farland LV, Shah DK, Harris HR, Kvaskoff M, Zondervan K, et al. Risk for and consequences of endometriosis: A critical epidemiologic review. *Best Pract Res Clin Obstet Gynaecol*. 2018;51:1–15.
- Saunders PTK, Horne AW. Endometriosis: Etiology, pathobiology, and therapeutic prospects. *Cell*. 2021;27(184):2807–24.
- Irving JA, Clement PB. Diseases of the peritoneum. In: Kurman RJ, editor. *Blaustein's pathology of the female genital tract*. 7th ed. New York: Springer-Verlag; 2018. p. 771–840.
- Stewart CJR, Ayhan A, Fukunaga M, Huntsman DG (2020). Endometriosis and related conditions. In: WHO Classification of Tumours Editorial Board, ed. *WHO classification of tumours female genital tumours*, 5th ed. Lyon: IARC Library Cataloguing-in-Publication Data:169–74.
- Prescott J, Farland LV, Tobias DK, Gaskins AJ, Spiegelman D, Chavarro JE, et al. A prospective cohort study of endometriosis and subsequent risk of infertility. *Hum Reprod*. 2016;31:1475–82.
- Kvaskoff M, Mu F, Terry KL, Harris HR, Poole EM, Farland L, Missmer SA. Endometriosis: a high-risk population for major chronic diseases? *Hum Reprod Update*. 2015;21:500–16.
- Sampson JA. Metastatic or Embolic Endometriosis, due to the Menstrual Dissemination of Endometrial Tissue into the Venous Circulation. *Am J Pathol*. 1927;3(93–110):43.
- Sampson JA. Peritoneal endometriosis due to menstrual dissemination of endometrial tissue into the peritoneal cavity. *Am J Obstet Gynecol*. 1927;14:422–69.
- Wiegand KC, Shah SP, Al-Agha OM, Zhao Y, Tse K, Zeng T, et al. ARID1A mutations in endometriosis associated ovarian carcinomas. *N Engl J Med*. 2010;363:1532–43.
- Vercellini P, Viganò P, Somigliana E, Fedele L. Endometriosis: pathogenesis and treatment. *Nat Rev Endocrinol*. 2014;10:261–75.
- Canis M, Donnez JG, Guzik DS, Halme JK, Rock JA, Schenken RS, Vernon MW. Revised American Society for Reproductive Medicine classification of endometriosis: 1996. *Fertil Steril*. 1997;67(5):817–21. [https://doi.org/10.1016/S0015-0282\(97\)81391-X](https://doi.org/10.1016/S0015-0282(97)81391-X).
- Johnson NP, Hummelshoj L, Adamson GD, Keckstein J, Taylor HS, Abrao MS, et al. World Endometriosis Society consensus on the classification of endometriosis. *Hum Reprod*. 2017;32:315–24.
- Kido A, Himoto Y, Moribata Y, Kurata Y, Nakamoto Y. MRI in the Diagnosis of Endometriosis and Related Diseases. *Korean J Radiol*. 2022;23:426–45.
- Keckstein J, Saridogan E, Ulrich UA, Sillem M, Oppelt P, Schweppe KW, et al. The #Enzian classification: A comprehensive non-invasive and surgical description system for endometriosis. *Acta Obstet Gynecol Scand*. 2021;100:1165–75.
- Di Paola V, Manfredi R, Castelli F, Negrelli R, Mehrabi S, Pozzi MR. Detection and localization of deep endometriosis by means of MRI and correlation with the ENZIAN score. *Eur J Radiol*. 2015;84:568–74.
- Burla L, Scheiner D, Samartzis EP, Seidel S, Eberhard M, Fink D, et al. The ENZIAN score as a preoperative MRI-based classification instrument for deep infiltrating endometriosis. *Arch Gynecol Obstet*. 2019;300:109–16.
- Thomassin-Naggara I, Lamrabet S, Crestani A, Bekhouche A, Wahab CA, Kermarrec E, et al. Magnetic resonance imaging classification of deep pelvic endometriosis: description and impact on surgical management. *Hum Reprod*. 2020;35:1589–600.
- Nishimura K, Togashi K, Itoh K, Fujisawa I, Noma S, Kawamura Y, et al. Endometrial cysts of the ovary: MR imaging. *Radiology*. 1987;162:315–8.
- Togashi K, Nishimura K, Kimura I, Tsuda Y, Yamashita K, Shibata T, et al. Endometrial cysts: diagnosis with MR imaging. *Radiology*. 1991;180:73–8.
- Dias JL, Veloso Gomes F, Lucas R, Cunha TM. The shading sign: is it exclusive of endometriomas? *Abdom Radiol*. 2015;40:2566–72.
- Glastonbury CM. The shading sign. *Radiology*. 2002;224:199–201.
- Corwin MT, Gerscovich EO, Lamba R, Wilson M, McGahan JP. Differentiation of ovarian endometriomas from hemorrhagic cysts at MR imaging: utility of the T2 dark spot sign. *Radiology*. 2014;271:126–32.
- Takeuchi M, Matsuzaki K, Kubo H, Nishitani H. Magnetic resonance manifestations of endometrial cysts at 3 T compared with 1.5 T. *J Comput Assist Tomogr*. 2008;32:369–71.
- Takeuchi M, Matsuzaki K, Nishitani H. Susceptibility-weighted MRI of endometrioma: preliminary results. *AJR Am J Roentgenol*. 2008;191:1366–70.
- Bulut E, Peker M, Kupeli A, Danisan G, Bulut AC. The efficiency of susceptibility-weighted MRI in the differentiation of endometriomas from haemorrhagic ovarian cysts. *Abdom Radiol*. 2021;46:5337–43.
- Cornillie FJ, Oosterlynck D, Lauweryns JM, Koninckx PR. Deeply infiltrating pelvic endometriosis: histology and clinical significance. *Fertil Steril*. 1990;53:978–83.
- Koninckx PR, Martin DC. Deep endometriosis: a consequence of infiltration or retraction or possibly adenomyosis externa? *Fertil Steril*. 1992;58:924–8.
- Jha P, Sakala M, Chamie LP, Feldman M, Hindman N, Huang C, et al. Endometriosis MRI lexicon: consensus statement from the society of abdominal radiology endometriosis disease-focused panel. *Abdom Radiol*. 2020;45:1552–68.
- Chamié LP, Blasbalg R, Pereira RM, Warmbrand G, Serafini PC. Findings of pelvic endometriosis at transvaginal US, MR imaging, and laparoscopy. *Radiographics*. 2011;31:E77-100.

31. Bazot M, Daraï E. Diagnosis of deep endometriosis: clinical examination, ultrasonography, magnetic resonance imaging, and other techniques. *Fertil Steril*. 2017;108:886–94.
32. Bazot M, Gasner A, Lafont C, Ballester M, Daraï E. Deep pelvic endometriosis: limited additional diagnostic value of postcontrast in comparison with conventional MR images. *Eur J Radiol*. 2011;80:e331–9.
33. Coutinho A Jr, Bittencourt LK, Pires CE, Junqueira F, Lima CM, Coutinho E, et al. MR imaging in deep pelvic endometriosis: a pictorial essay. *Radiographics*. 2011;31:549–67.
34. Bazot M, Daraï E, Hourani R, Thomassin I, Cortez A, Uzan S, et al. Deep pelvic endometriosis: MR imaging for diagnosis and prediction of extension of disease. *Radiology*. 2004;232:379–89.
35. Del Frate C, Girometti R, Pittino M, Del Frate G, Bazzocchi M, Zuiani C. Deep retroperitoneal pelvic endometriosis: MR imaging appearance with laparoscopic correlation. *Radiographics*. 2006;26:1705–18.
36. Cimsit C, Yoldemir T, Guclu M, Akpinar IN. Susceptibility-weighted magnetic resonance imaging for the evaluation of deep infiltrating endometriosis: preliminary results. *Acta Radiol*. 2016;57:878–85.
37. Kataoka ML, Togashi K, Yamaoka T, Koyama T, Ueda H, Kobayashi H, et al. Posterior cul-de-sac obliteration associated with endometriosis: MR imaging evaluation. *Radiology*. 2005;234:815–23.
38. Macario S, Chassang M, Novellas S, Baudin G, Delotte J, Toullalan O, et al. The value of pelvic MRI in the diagnosis of posterior cul-de-sac obliteration in cases of deep pelvic endometriosis. *AJR Am J Roentgenol*. 2012;199:1410–5.
39. Williams JC, Burnett TL, Jones T, Venkatesh SK, VanBuren WM. Association between kissing and repositioned ovaries and severity of endometriosis: MR imaging evaluation. *Abdom Radiol*. 2020;45:1637–44.
40. Härmä K, Binda A, Ith M, Poellinger A, Siegenthaler F, Heverhagen J, et al. Cloverleaf Sign in Pelvic Magnetic Resonance Imaging for Deep Infiltrating Endometriosis: Association With Longer Operation Times, Greater Blood Loss, and Higher Rates of Bowel Resection. *Invest Radiol*. 2020;55:53–9.
41. Chamié LP, Ribeiro DMFR, Tiferes DA, Macedo Neto AC, Serafini PC. Atypical Sites of Deeply Infiltrative Endometriosis: Clinical Characteristics and Imaging Findings. *Radiographics*. 2018;38:309–28.
42. Gui B, Valentini AL, Ninivaggi V, Marino M, Iacobucci M, Bonomo L. Deep pelvic endometriosis: don't forget round ligaments. Review of anatomy, clinical characteristics, and MR imaging features. *Abdom Imaging*. 2014;39:622–32.
43. Tokue H, Tsushima Y, Endo K. Magnetic resonance imaging findings of extrapelvic endometriosis of the round ligament. *Jpn J Radiol*. 2009;27:45–7.
44. Chapron C, Tosti C, Marcellin L, Bourdon M, Lafay-Pillet MC, Millischer AE, et al. Relationship between the magnetic resonance imaging appearance of adenomyosis and endometriosis phenotypes. *Hum Reprod*. 2017;32:1393–401.
45. Kishi Y, Suginami H, Kuramori R, Yabuta M, Suginami R, Taniguchi F. Four subtypes of adenomyosis assessed by magnetic resonance imaging and their specification. *Am J Obstet Gynecol*. 2012;207(114):e1–7.
46. Takeuchi M, Matsuzaki K. Adenomyosis: usual and unusual imaging manifestations, pitfalls, and problem-solving MR imaging techniques. *Radiographics*. 2011;31:99–115.
47. Busard MP, Mijatovic V, Lüchinger AB, Bleeker MC, Pieters van den Bos IC, Schats R, et al. MR imaging of bladder endometriosis and its relationship with the anterior uterine wall: experience in a tertiary referral centre. *Eur J Radiol*. 2012;81:2106–11.
48. Tian Z, Zhang YC, Sun XH, Wang Y, Zhao Y, Chang XH, et al. Accuracy of transvaginal ultrasound and magnetic resonance imaging for diagnosis of deep endometriosis in bladder and ureter: a meta-analysis. *J Obstet Gynaecol*. 2022;42:2272–81.
49. Takeuchi M, Matsuzaki K, Harada M. Susceptibility-weighted MRI of extra-ovarian endometriosis: preliminary results. *Abdom Imaging*. 2015;40:2512–6.
50. Busard MP, van der Houwen LE, Bleeker MC, Pieters van den Bos IC, Cuesta MA, van Kuijk C, et al. Deep infiltrating endometriosis of the bowel: MR imaging as a method to predict muscular invasion. *Abdom Imaging*. 2012;37:549–57.
51. Yoon JH, Choi D, Jang KT, Kim CK, Kim H, Lee SJ, et al. Deep rectosigmoid endometriosis: “mushroom cap” sign on T2-weighted MR imaging. *Abdom Imaging*. 2010;35:726–33.
52. Jaramillo-Cardoso A, Shenoy-Bhangle AS, VanBuren WM, Schiappacasse G, Menias CO, Morteale KJ. Imaging of gastrointestinal endometriosis: what the radiologist should know. *Abdom Radiol*. 2020;45:1694–710.
53. Li J, Liu Y, Du K, Xiao L, He X, Dai F, et al. Endometriosis in para-aortic lymph node resembling a malignancy: a case report and literature review. *BMC Womens Health*. 2022;22:101.
54. Beavis AL, Matsuo K, Grubbs BH, Srivastava SA, Truong CM, Moffitt MN, et al. Endometriosis in para-aortic lymph nodes during pregnancy: case report and review of literature. *Fertil Steril*. 2011;95(2429):e9–13.
55. Yarmish G, Sala E, Goldman DA, Lakhman Y, Soslow RA, Hricak H, et al. Abdominal wall endometriosis: differentiation from other masses using CT features. *Abdom Radiol*. 2017;42:1517–23.
56. Jaramillo-Cardoso A, Balcacer P, Garces-Descovich A, Beker K, Roth E, Glickman J, Morteale KJ. Multimodality imaging and clinicopathologic assessment of abdominal wall endometriosis: knocking down the enigma. *Abdom Radiol*. 2020;45:1800–12.
57. Busard MP, Mijatovic V, van Kuijk C, Hompes PG, van Waesberghe JH. Appearance of abdominal wall endometriosis on MR imaging. *Eur Radiol*. 2010;20:1267–76.
58. Solak A, Sahin N, Genç B, Sever AR, Genç M, Sivriköz ON. Diagnostic value of susceptibility-weighted imaging of abdominal wall endometriomas during the cyclic menstrual changes: a preliminary study. *Eur J Radiol*. 2013;82:e411–6.
59. Rousset P, Gregory J, Rousset-Jablonski C, Hugon-Rodin J, Regnard JF, Chapron C, et al. MR diagnosis of diaphragmatic endometriosis. *Eur Radiol*. 2016;26:3968–77.
60. Gil Y, Tulandi T. Diagnosis and Treatment of Catamenial Pneumothorax: A Systematic Review. *J Minim Invasive Gynecol*. 2020;27:48–53.
61. Joseph J, Sahn SA. Thoracic endometriosis syndrome: new observations from an analysis of 110 cases. *Am J Med*. 1996;100:164–70.
62. Suzuki S, Yasumoto M, Matsumoto R, Andoh A. MR findings of ruptured endometrial cyst: comparison with tubo-ovarian abscess. *Eur J Radiol*. 2012;81:3631–7.
63. Iraha Y, Okada M, Iraha R, Azama K, Yamashiro T, Tsubakimoto M, et al. CT and MR Imaging of Gynecologic Emergencies. *Radiographics*. 2017;37:1569–86.
64. Chen MJ, Yang JH, Yang YS, Ho HN. Increased occurrence of tubo-ovarian abscesses in women with stage III and IV endometriosis. *Fertil Steril*. 2004;82:498–9.
65. Revzin MV, Mathur M, Dave HB, Macer ML, Spektor M. Pelvic Inflammatory Disease: Multimodality Imaging Approach with Clinical-Pathologic Correlation. *Radiographics*. 2016;36:1579–96.
66. Jain KA. Imaging of peritoneal inclusion cysts. *AJR Am J Roentgenol*. 2000;174:1559–63.

67. Robinson KA, Menias CO, Chen L, Schiappacasse G, Shaaban AM, Caserta MP, et al. Understanding malignant transformation of endometriosis: imaging features with pathologic correlation. *Abdom Radiol*. 2020;45:1762–75.
68. Sampson JA. Endometrial carcinoma of the ovary, arising in endometrial tissue in that organ. *Arch Surg*. 1925;10:1–72.
69. Scott RB. Malignant changes in endometriosis. *Obstet Gynecol*. 1953;2:283–9.
70. Grandi G, Toss A, Cortesi L, Botticelli L, Volpe A, Cagnacci A. The Association between Endometriomas and Ovarian Cancer: Preventive Effect of Inhibiting Ovulation and Menstruation during Reproductive Life. *Biomed Res Int*. 2015;2015: 751571.
71. Yamaguchi K, Mandai M, Toyokuni S, Hamanishi J, Higuchi T, Takakura K, et al. Contents of endometriotic cysts, especially the high concentration of free iron, are a possible cause of carcinogenesis in the cysts through the iron-induced persistent oxidative stress. *Clin Cancer Res*. 2008;14:32–40.
72. Wang C, Liang Z, Liu X, Zhang Q, Li S. The association between endometriosis, tubal ligation, hysterectomy and epithelial ovarian cancer: meta-analyses. *Int J Environ Res Public Health*. 2016;13:E1138.
73. Murakami K, Kotani Y, Nakai H, Matsumura N. Endometriosis-Associated Ovarian Cancer: The Origin and Targeted Therapy. *Cancers*. 2020;12:1676.
74. Higashiura Y, Kajihara H, Shigetomi H, Kobayashi H. Identification of multiple pathways involved in the malignant transformation of endometriosis (Review). *Oncol Lett*. 2012;4:3–9.
75. Wendel JRH, Wang X, Hawkins SM. The Endometriotic Tumor Microenvironment in Ovarian Cancer. *Cancers*. 2018;10:261.
76. Tanaka YO, Yoshizako T, Nishida M, Yamaguchi M, Sugimura K, Itai Y. Ovarian carcinoma in patients with endometriosis: MR imaging findings. *AJR Am J Roentgenol*. 2000;175:1423–30.
77. Takeuchi M, Matsuzaki K, Uehara H, Nishitani H. Malignant transformation of pelvic endometriosis: MR imaging findings and pathologic correlation. *Radiographics*. 2006;26:407–17.
78. Tanaka YO, Okada S, Yagi T, Satoh T, Oki A, Tsunoda H, et al. MRI of endometriotic cysts in association with ovarian carcinoma. *AJR Am J Roentgenol*. 2010;194:355–61.
79. Takeuchi M, Matsuzaki K, Nishitani H. Diffusion-weighted magnetic resonance imaging of ovarian tumors: differentiation of benign and malignant solid components of ovarian masses. *J Comput Assist Tomogr*. 2010;34:173–6.
80. Nishio N, Kido A, Kataoka M, Kuwahara R, Nakao K, Kurata Y, et al. Longitudinal changes in magnetic resonance imaging of malignant and borderline tumors associated with ovarian endometriotic cyst comparing with endometriotic cysts without arising malignancy. *Eur J Radiol*. 2018;105:175–81.
81. McDermott S, Oei TN, Iyer VR, Lee SI. MR imaging of malignancies arising in endometriomas and extraovarian endometriosis. *Radiographics*. 2012;32:845–63.
82. Kataoka M, Togashi K, Koyama T, Yamaoka T, Iwasa Y, Fujii S, et al. MR imaging of müllerian mucinous borderline tumors arising from endometriotic cysts. *J Comput Assist Tomogr*. 2002;26:532–7.
83. Kurata Y, Kido A, Moribata Y, Kameyama K, Himoto Y, Minamiguchi S, et al. Diagnostic performance of MR imaging findings and quantitative values in the differentiation of seromucinous borderline tumour from endometriosis-related malignant ovarian tumour. *Eur Radiol*. 2017;27:1695–703.
84. Kurata Y, Kido A, Moribata Y, Kameyama K, Minamiguchi S, Konishi I, et al. Differentiation of Seromucinous Borderline Tumor from Serous Borderline Tumor on MR Imaging. *Magn Reson Med Sci*. 2018;17:211–7.
85. Arslanian E, Singh K, James Sung C, Qudus MR. Somatic mutation analysis of Mesonephric-Like adenocarcinoma and associated putative precursor Lesions: Insight into pathogenesis and potential molecular treatment targets. *Gynecol Oncol Rep*. 2022;42: 101049.
86. Seay K, Akanbi T, Bustamante B, Chaudhary S, Goldberg GL. Mesonephric-like adenocarcinoma of the ovary with co-existent endometriosis: A case report and review of the literature. *Gynecol Oncol Rep*. 2020;34: 100657.
87. Saida T, Mori K, Tanaka YO, Sakai M, Amano T, Kikuchi S, et al. Carcinosarcoma of the ovary: MR and clinical findings compared with high-grade serous carcinoma. *Jpn J Radiol*. 2021;39:357–66.
88. Shetty M, Lal N, Vu NH. Müllerian adenosarcoma of the ovary: case report and review of the literature. *Ultrasound Q*. 2007;23:189–91.
89. Sqalli Houssaini M, Haloua M, Mourabiti AY, Tahiri L, Fdili Alaoui FZ, et al. A case of ovarian endometrial stromal sarcoma: Radiological and histopathological findings. *Radiol Case Rep*. 2023;28(18):3529–34.
90. Yamamoto S, Tsuda H, Suzuki K, Takano M, Tamai S, Matsumura O. An allelotype analysis indicating the presence of two distinct ovarian clear-cell carcinogenic pathways: endometriosis-associated pathway vs. clear-cell adenofibroma-associated pathway. *Virchows Arch*. 2009;455:261–70.
91. Zhao C, Wu LS, Barner R. Pathogenesis of ovarian clear cell adenofibroma, atypical proliferative (borderline) tumor, and carcinoma: clinicopathologic features of tumors with endometriosis or adenofibromatous components support two related pathways of tumor development. *J Cancer*. 2011;2:94–106.
92. Takeuchi M, Matsuzaki K, Uehara H, Furumoto H, Harada M. Clear cell adenocarcinoma arising from clear cell adenofibroma of the ovary: value of DWI and DCE-MRI. *Magn Reson Med Sci*. 2013;12:305–8.
93. Takeuchi M, Matsuzaki K, Nishitani H. Magnetic resonance manifestations of decidualized endometriomas during pregnancy. *J Comput Assist Tomogr*. 2008;32:353–5.
94. Morisawa N, Kido A, Kataoka M, Minamiguchi S, Konishi I, et al. Magnetic resonance imaging manifestations of decidualized endometriotic cysts: comparative study with ovarian cancers associated with endometriotic cysts. *J Comput Assist Tomogr*. 2014;38:879–84.
95. Takeuchi M, Matsuzaki K, Harada M. Computed diffusion-weighted imaging for differentiating decidualized endometrioma from ovarian cancer. *Eur J Radiol*. 2016;85:1016–9.
96. Ando T, Kato H, Kawaguchi M, Furui T, Morishige KI, Hyodo F, et al. MR findings for differentiating decidualized endometriomas from seromucinous borderline tumors of the ovary. *Abdom Radiol*. 2020;45:1783–9.
97. Parker RL, Dadmanesh F, Young RH, Clement PB. Polypoid endometriosis: a clinicopathologic analysis of 24 cases and a review of the literature. *Am J Surg Pathol*. 2004;28:285–97.
98. Takeuchi M, Matsuzaki K, Bando Y, Harada M. Magnetic resonance imaging characteristics of polypoid endometriosis and review of the literature. *J Obstet Gynaecol Res*. 2022;48:2583–93.
99. Takeuchi M, Matsuzaki K, Furumoto H, Nishitani H. Case report: A case of polypoid endometriosis: MR pathological correlation. *Br J Radiol*. 2008;81:e118–9.
100. Takeuchi M, Matsuzaki K, Bando Y, Nishimura M, Yoneda A, Harada M. A case of polypoid endometriosis with malignant transformation. *Abdom Radiol*. 2016;41:1699–702.